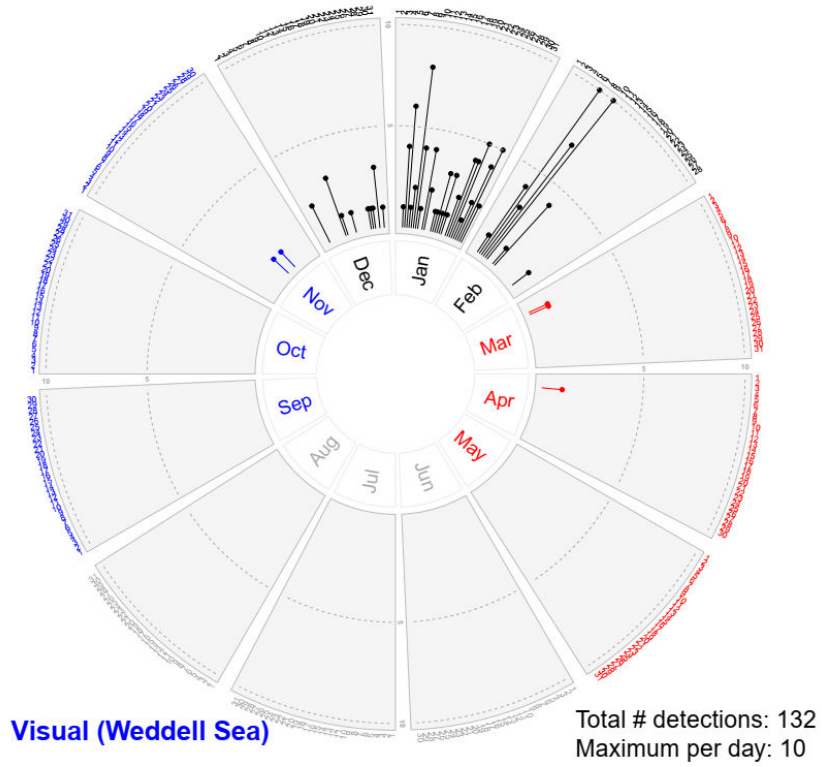
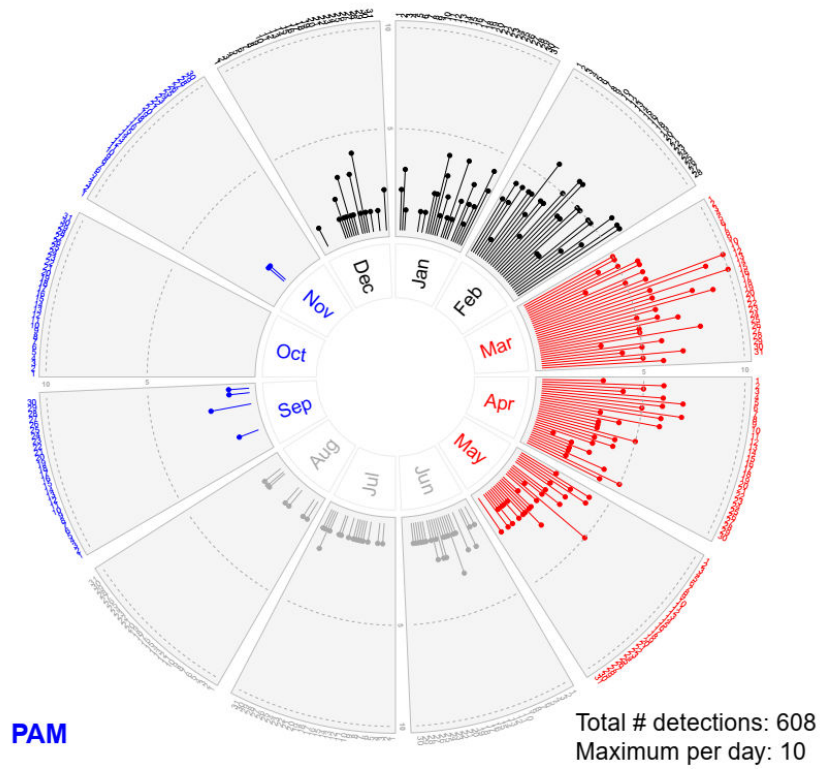


Supplementary materials for:

El-Gabbas A, Thomisch K, Van Opzeeland I, Burkhardt E, Boebel O (2023) **Dynamic species distribution models of Antarctic blue whales in the Weddell Sea using visual sighting and passive acoustic monitoring data.** Diversity and Distributions. <https://doi.org/10.1111/ddi.13790>



(A)



(B)

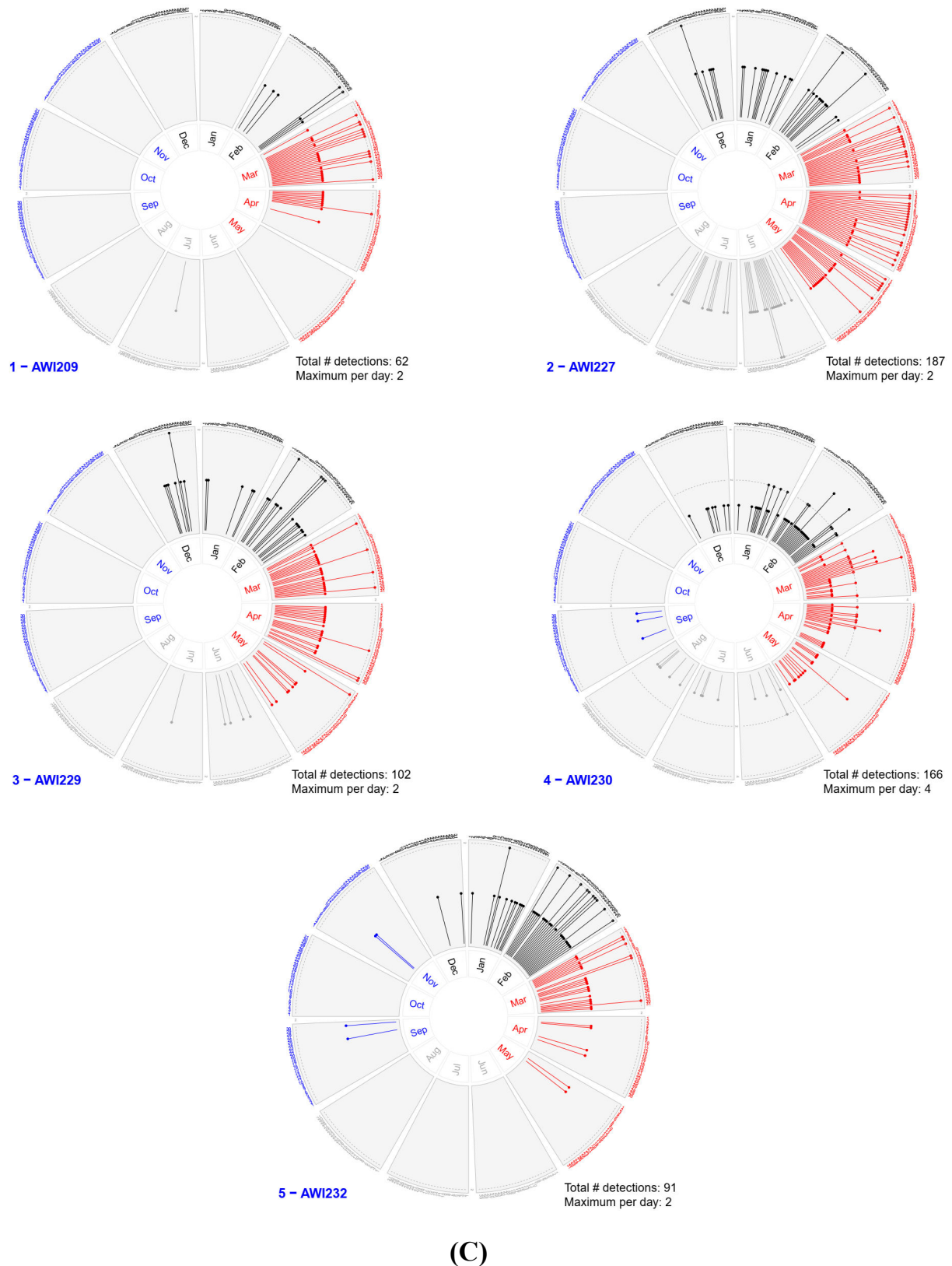


Figure S1: Temporal distribution of Antarctic blue whale detections.

Plots show the number of daily detections per calendar day (**A**: visual sightings (2003-2019) from the Weddell Sea; **B**: acoustic detections at the five stations; **C**: acoustic detections at each of the five stations). Most visual data were observed from December to mid-February (with only a single sighting in late February, two in March, one in April, and two in November).

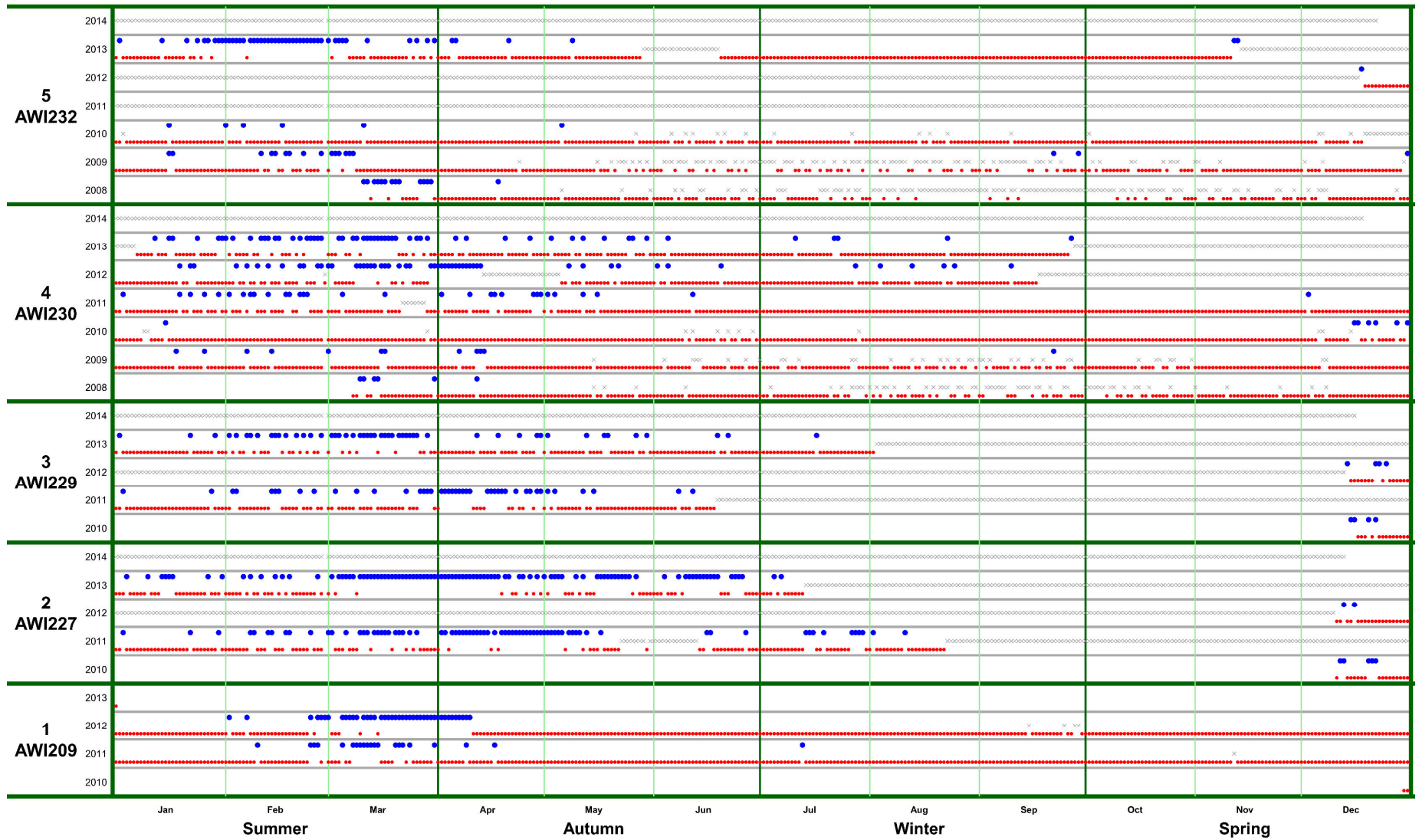


Figure S2: Year-round distribution of Antarctic blue whales’ acoustic detections (blue) and non-detections (red), grouped by station ID and year. Grey x symbols represent days with no acoustic data (e.g., due to device failure).

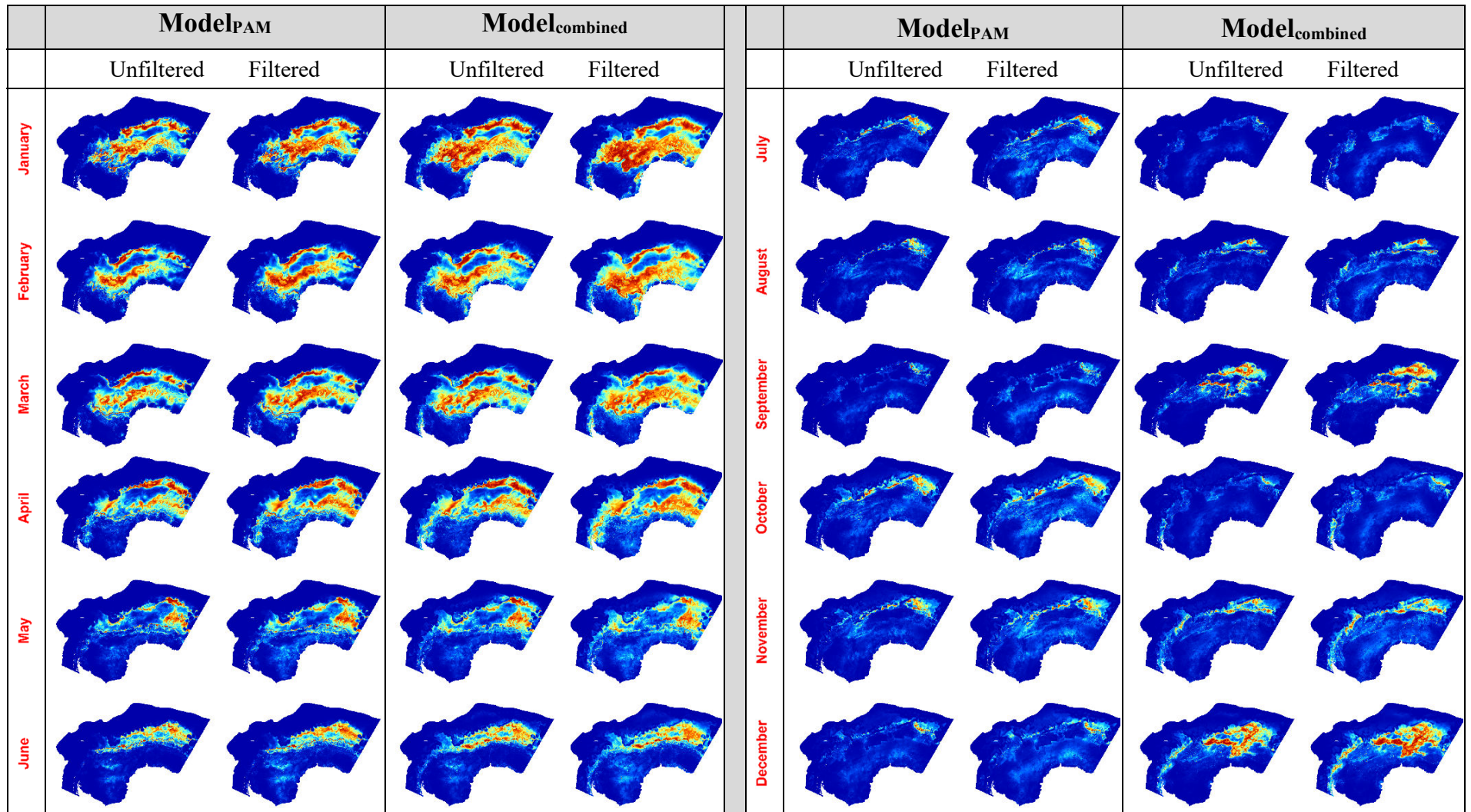
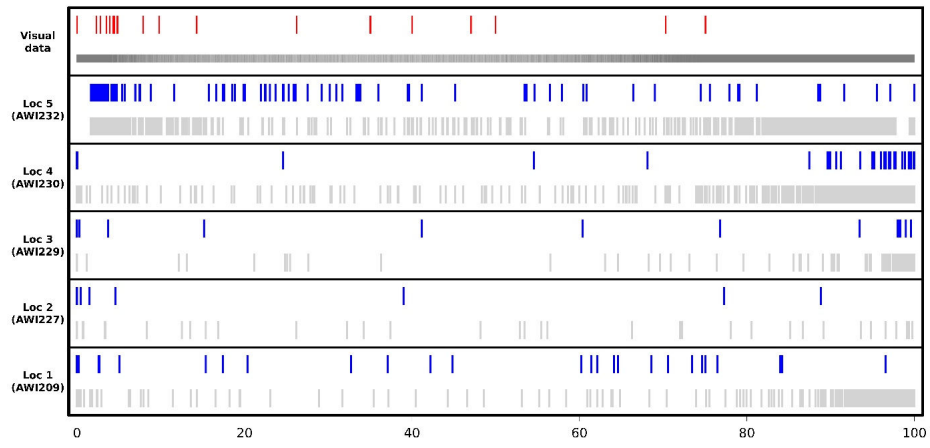
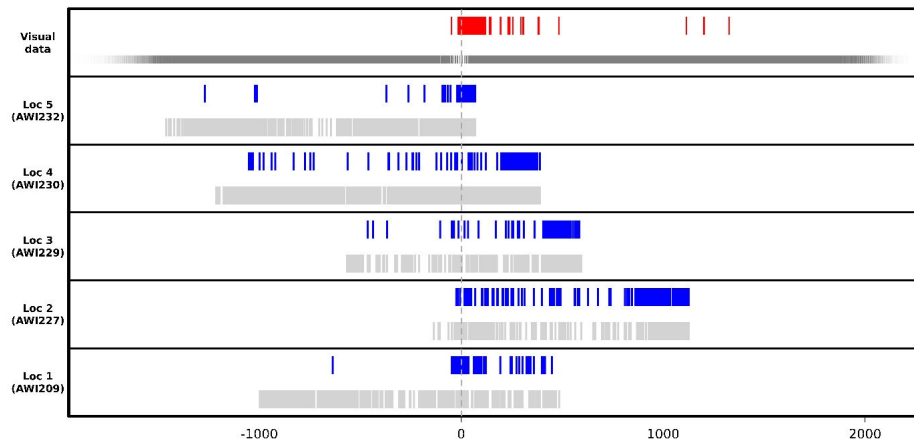


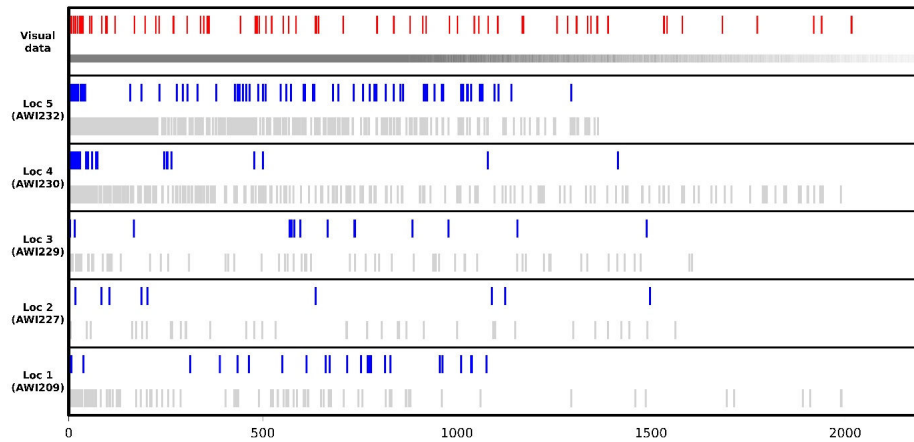
Figure S3: A comparison between predicted habitat suitability of Model_{PAM} and Model_{combined} using the unfiltered (daily) or temporally-filtered (using a single acoustic presence per 3-days interval) acoustic presences. Each map shows predicted habitat suitability on the 15th of each month in 2013.



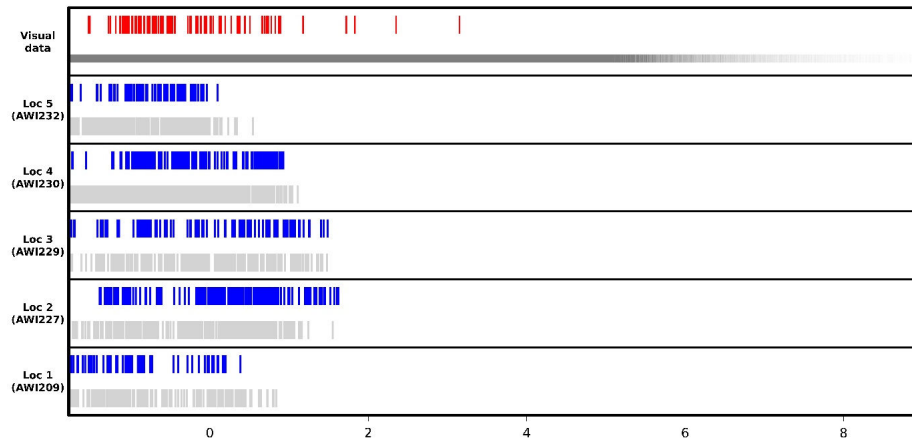
a) sea ice concentration



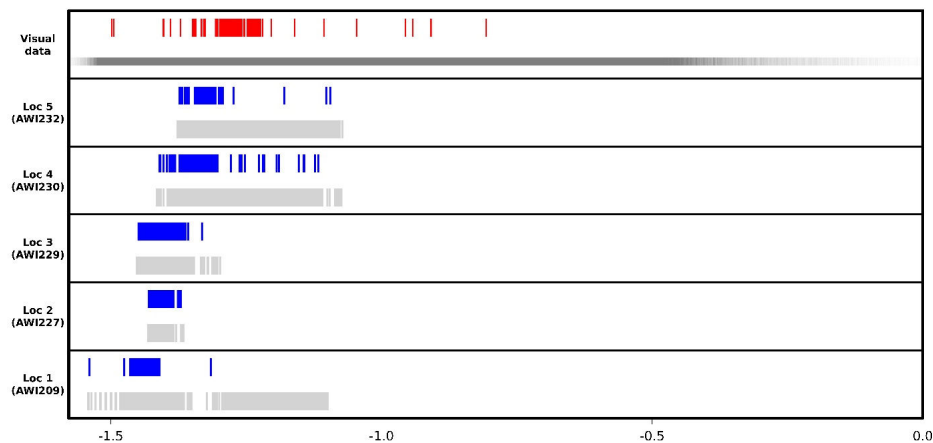
b) distance to the sea ice edge



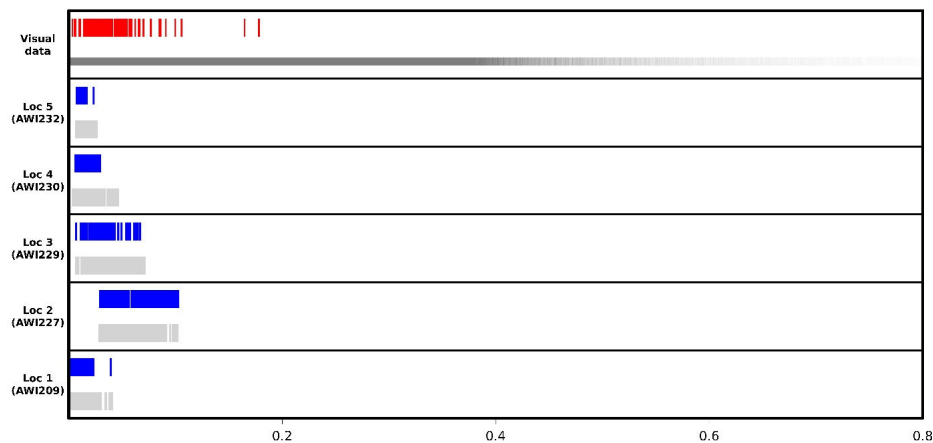
c) lagged sea ice



d) sea surface temperature



e) sea surface height



f) current speed

Figure S4: Predictors' values at visual and PAM dataset. In each plot, the bottom five rows show the predictor's value at each acoustic station, with days with acoustic presences marked with blue bars and days with no acoustic detections in light grey bars. In the top row, red bars represent values at visual sightings, while dark grey shows the distribution of the values of the respective predictor in the background information. See Figure 1 and Table 1 for more information on the PAM data.

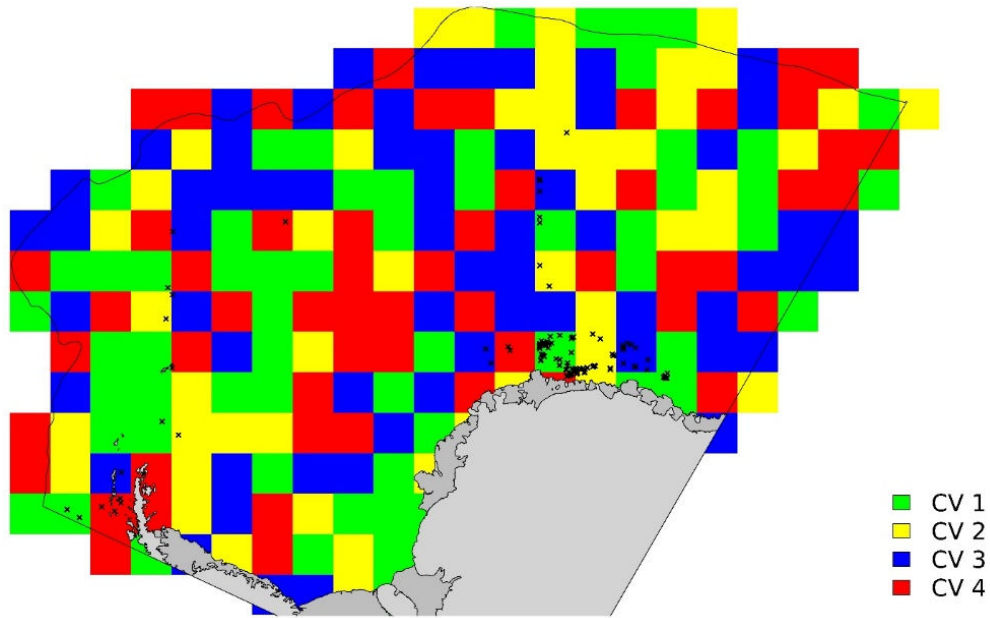
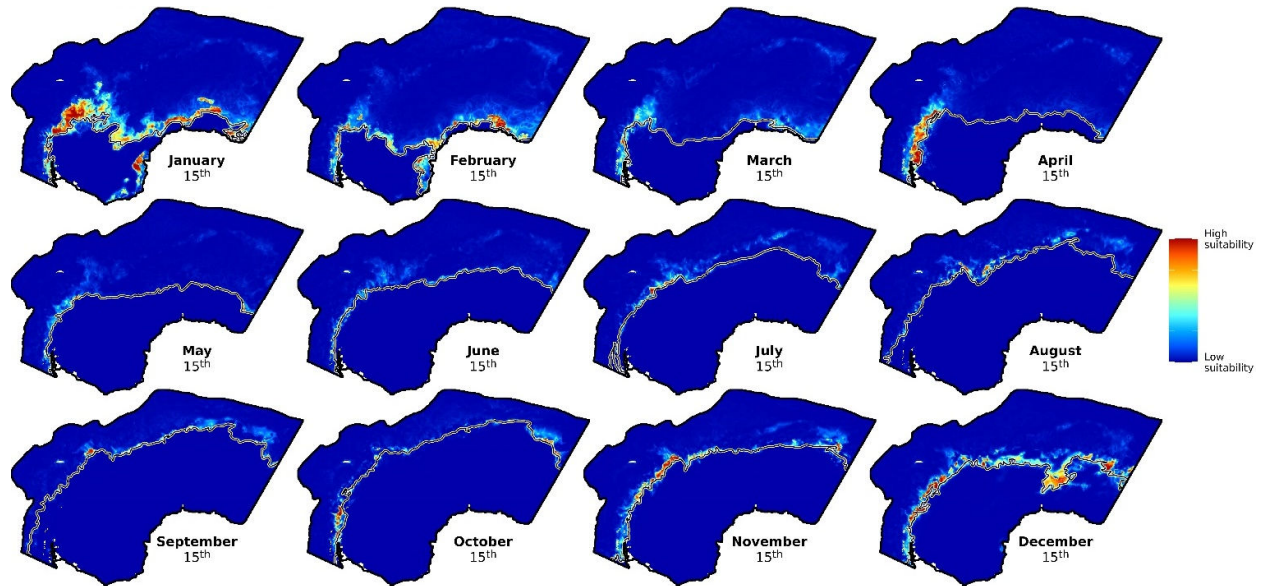
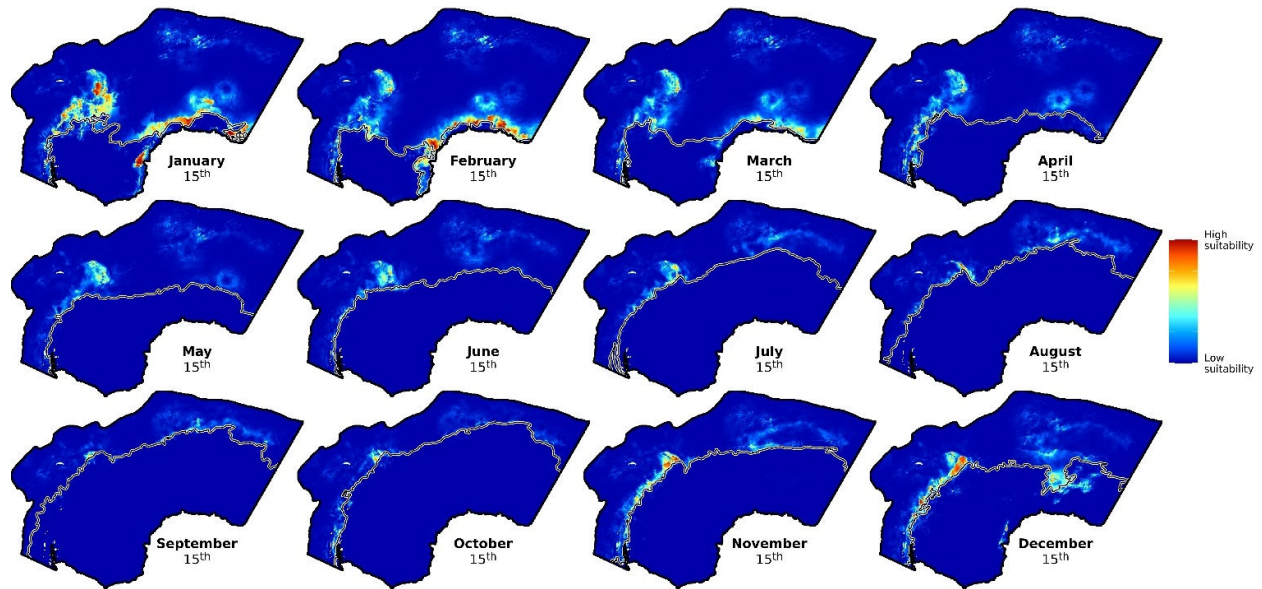


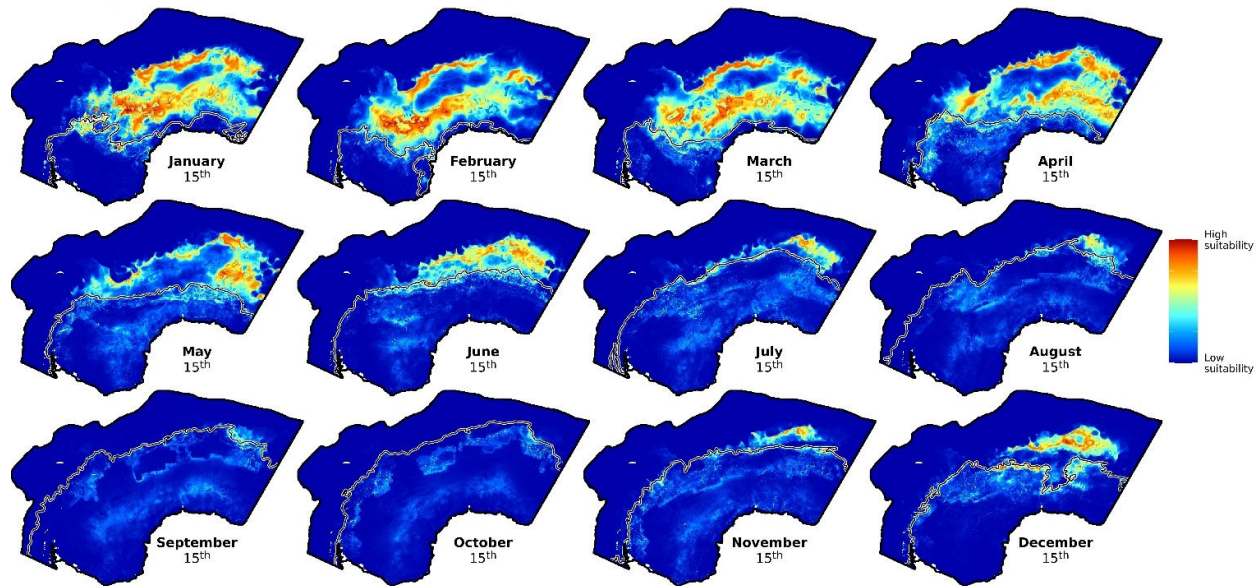
Figure S5: Spatial blocks used to cross-validate the visual data models ($\text{Model}_{\text{visual}}$). The study area is divided into larger blocks, each consisting of 25×25 cells (250×250 km). Blocks were distributed into four cross-validation folds (different colors). Antarctic blue whales' sightings (2003-2019) are shown in black dots.



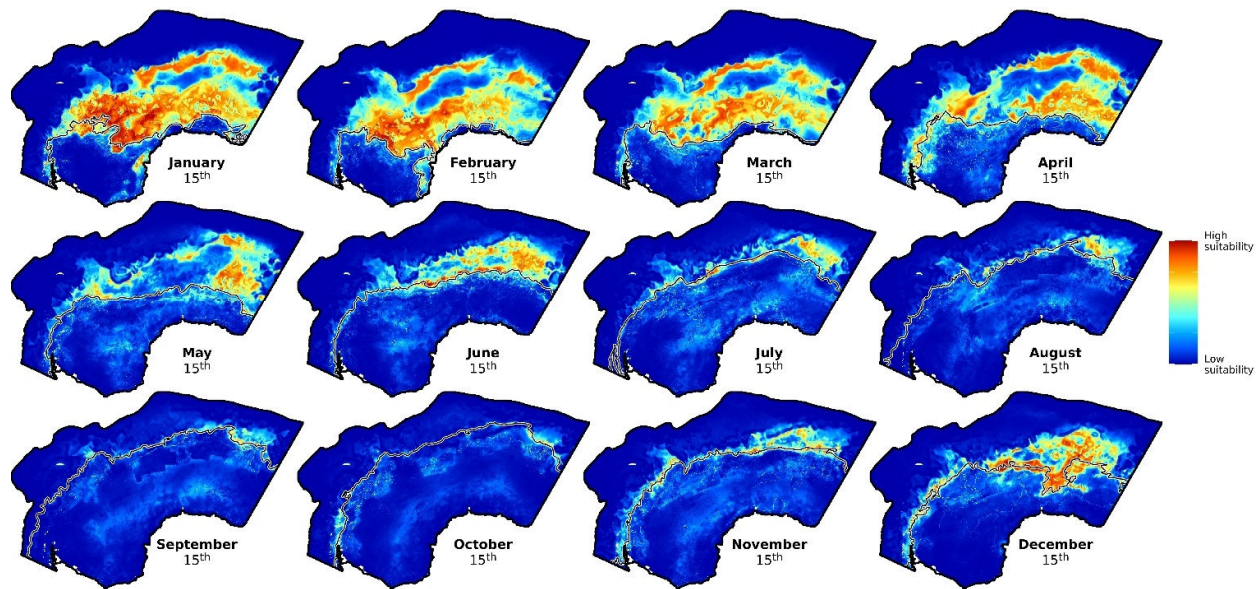
a) Visual-data models
Only dynamic predictors (this study)



b) Visual-data models
Circumpolar models, with both static and dynamic predictors (El-Gabbas et al. 2021a)



c) PAM-data models



d) Combined-data models

Figure S6: Examples of Antarctic blue whales' predicted habitat suitability on the 15th day of each month in 2013. Black lines represent the estimated location of the sea ice edge in the respective day.

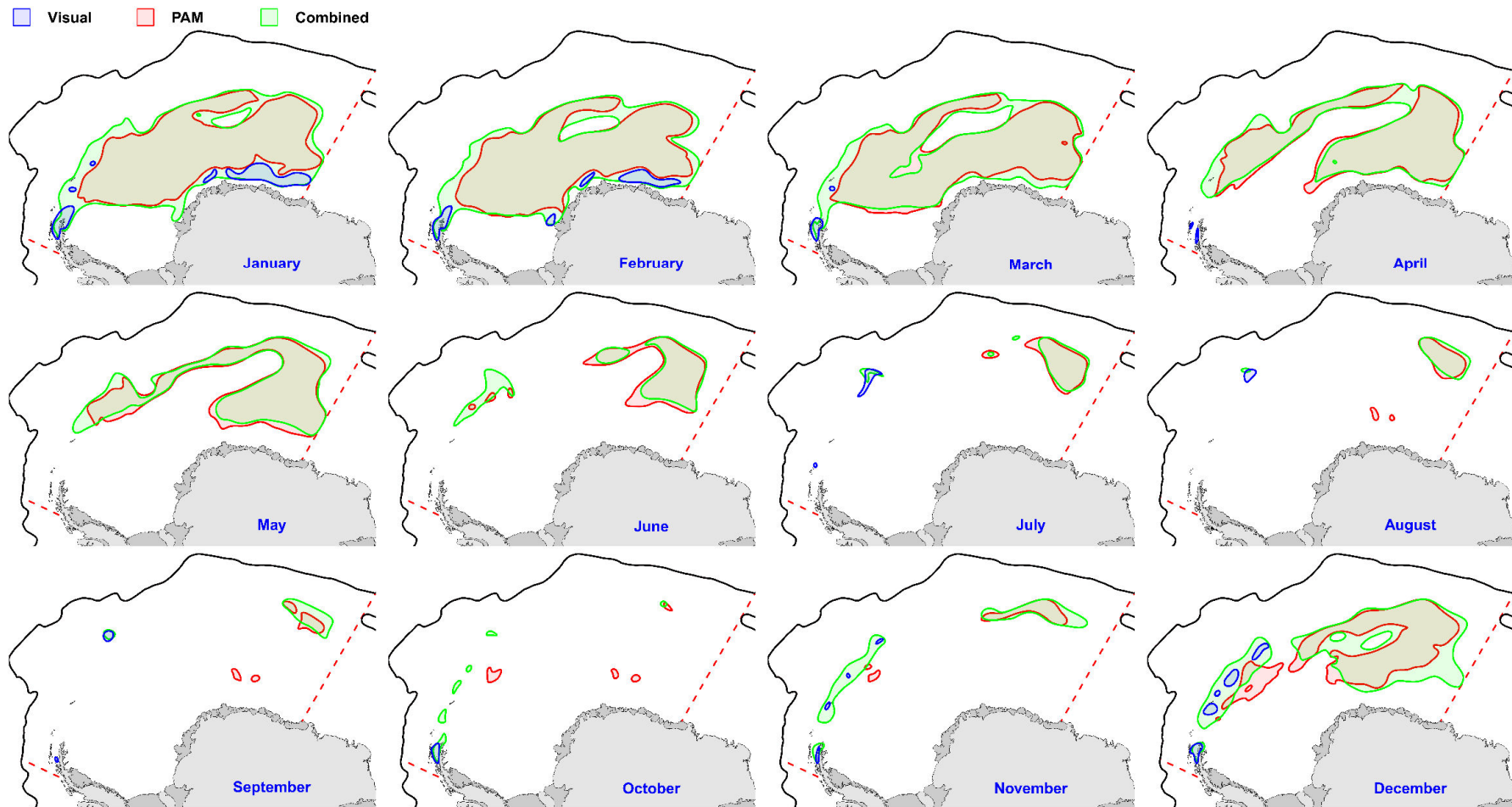
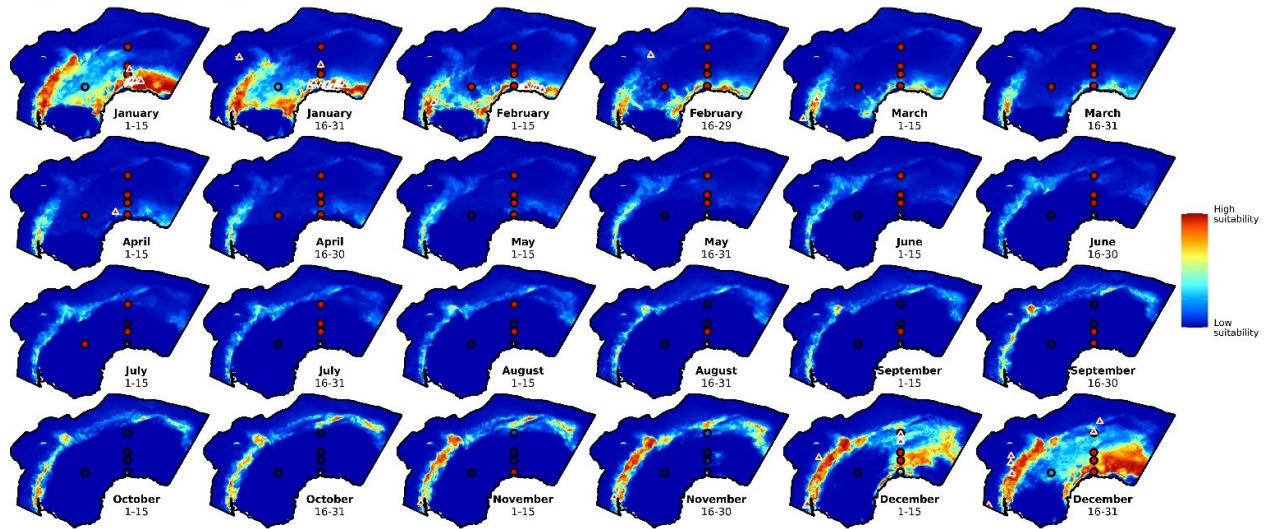
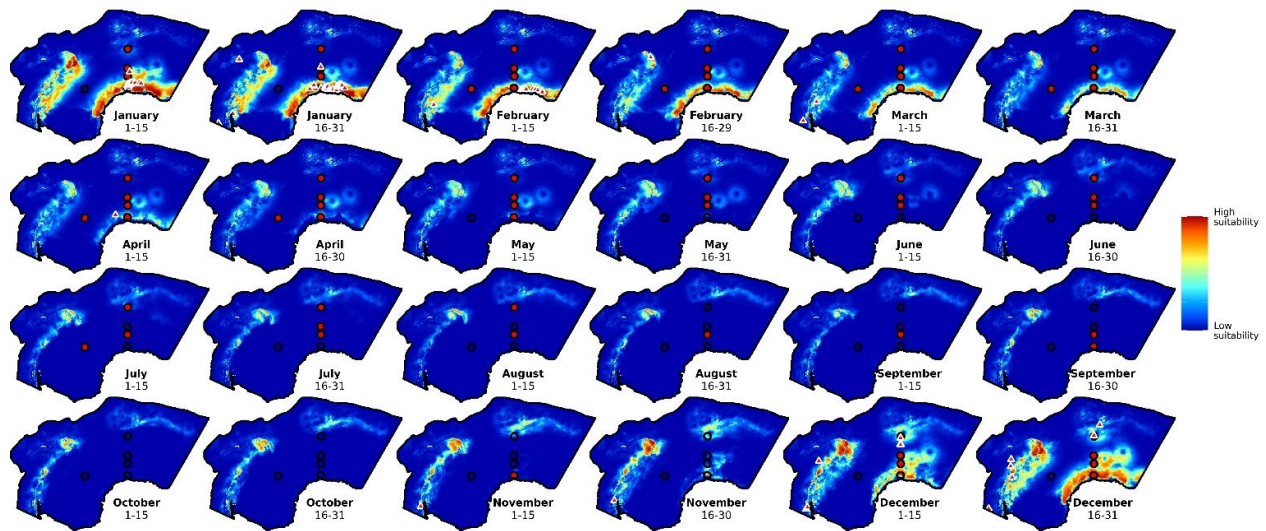


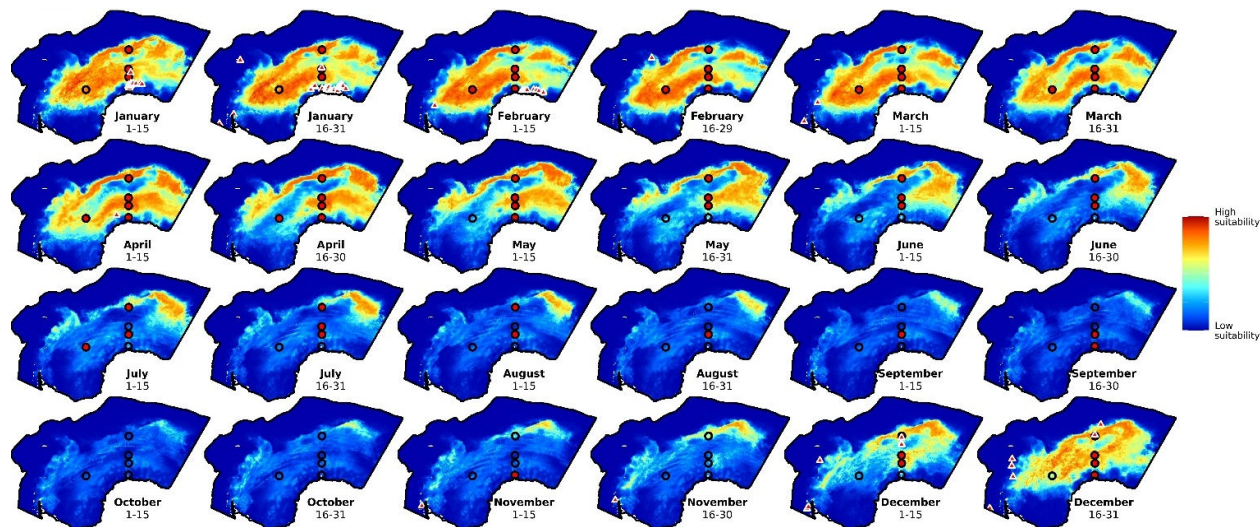
Figure S7: Overlap between monthly suitable habitats of the Antarctic blue whales in the Weddell Sea using the three model types. Daily suitable habitats (2003-2019) were identified using the model-specific threshold that maximizes the sum of sensitivity and specificity. Cells were identified as suitable on a particular day if they were predicted to be suitable in more than half of the cross-validated models. Daily suitable habitats were then summed in the respective month, and cells were identified as suitable if these cells were predicted to be suitable in $\geq 25\%$ of days in the respective month. Cells representing monthly suitable habitats were converted to polygons and smoothed to represent the overall pattern of suitable habitats in the respective month. Note that small polygons (with areas less than 1000 km^2) were removed from the plots to make the comparisons easy.



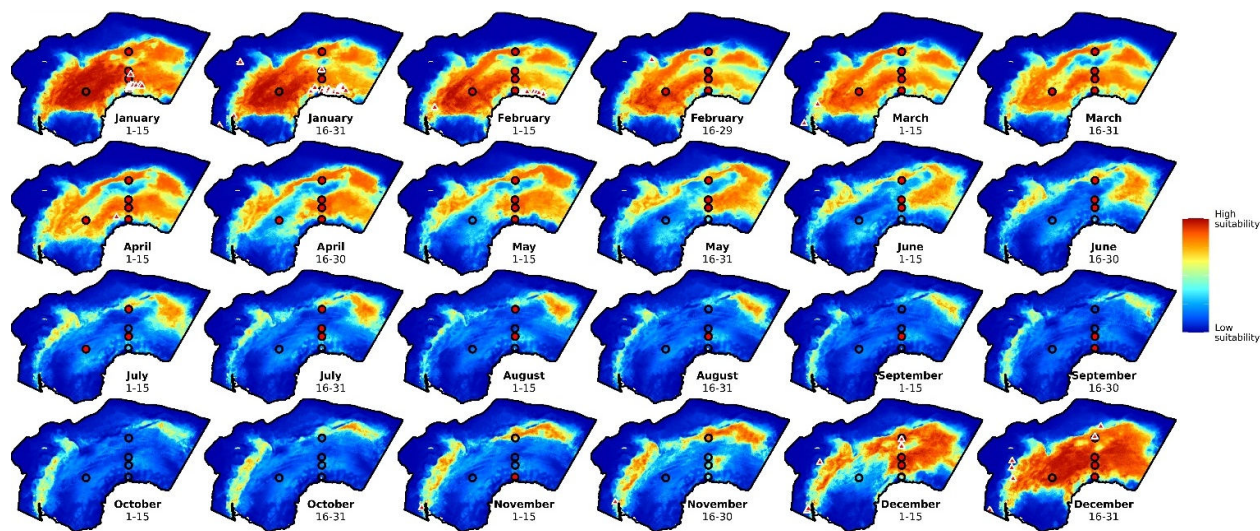
a) Visual-data models
Only dynamic predictors (this study)



b) Visual-data models
Circumpolar models, with both static and dynamic predictors (El-Gabbas et al. 2021a)



c) PAM-data models



d) Combined-data models

Figure S8: Biweekly summary of predicted habitat suitability of Antarctic blue whales of the four model types implemented. Each map shows the 90th quantile of daily predicted habitat suitability in the respective two-weeks period and model type from 2003 to 2019. Black circles indicate the location of PAM recorders. These circles are filled with red color if there are any acoustic presences in the respective two-weeks period. Red triangles show visual sightings in the respective two-weeks period. Monthly summary maps are shown in Figure 3. Examples of daily habitat suitability maps on the 15th day of each month in 2013 are shown in Figure S6.

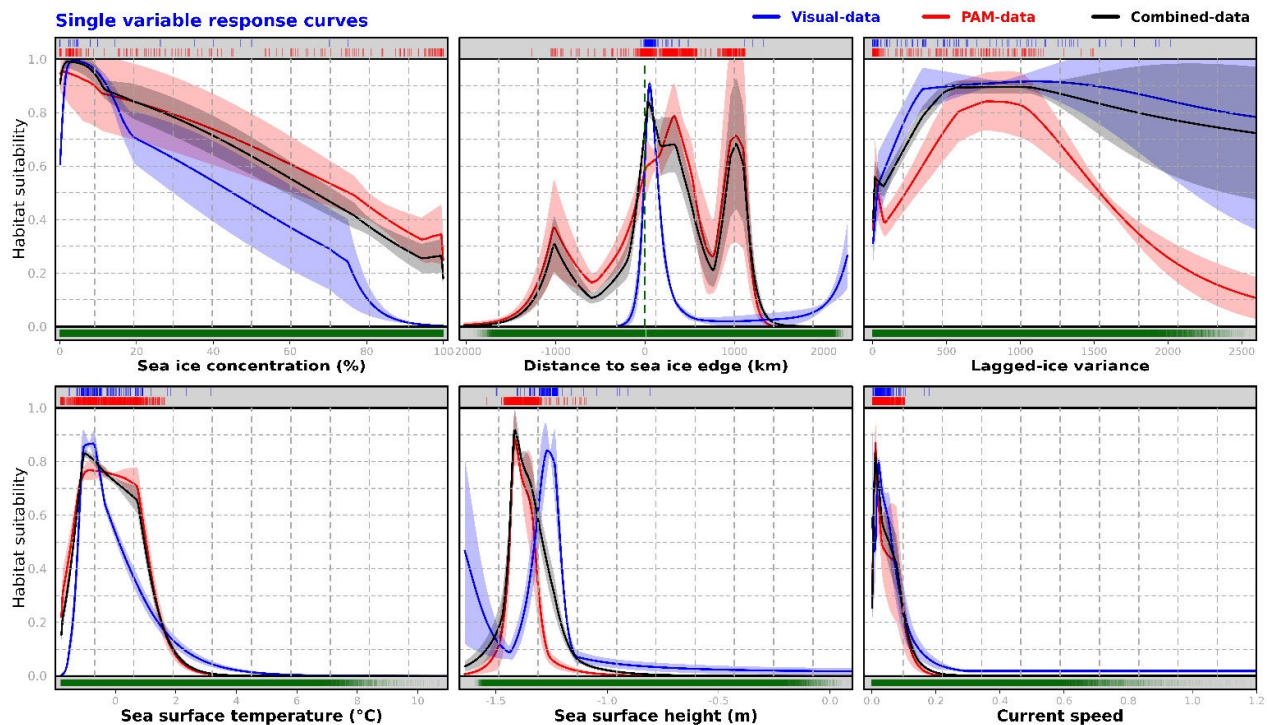
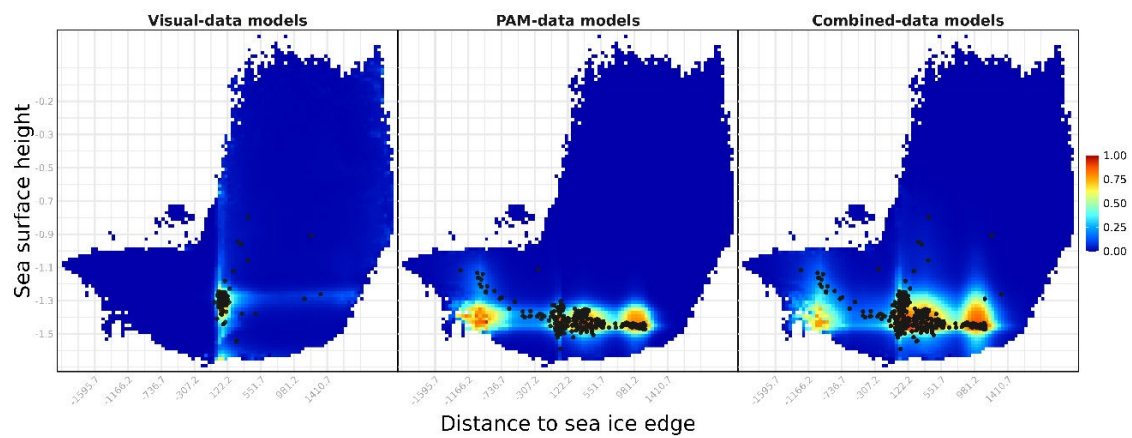
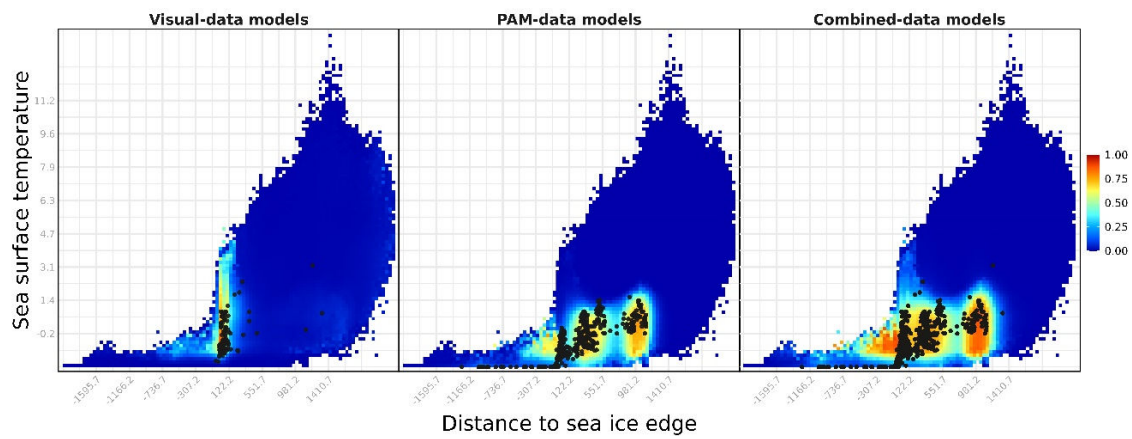
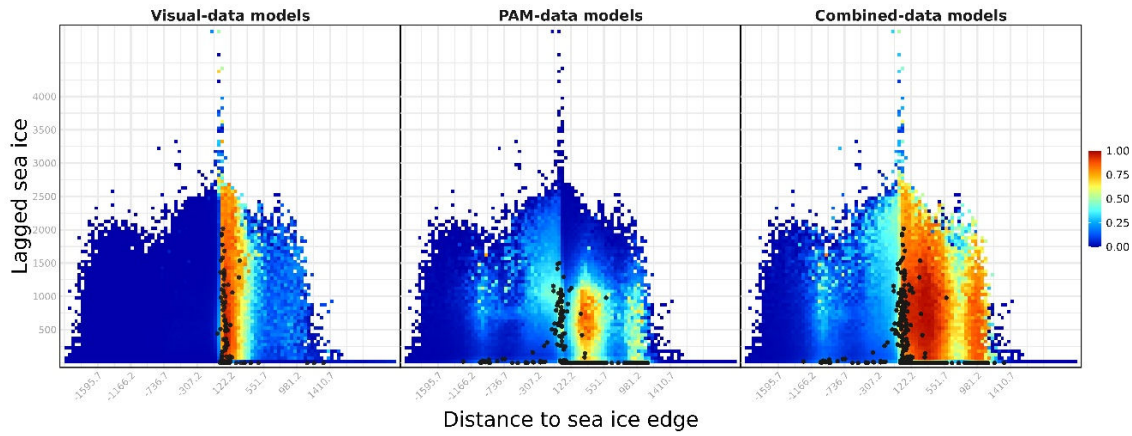
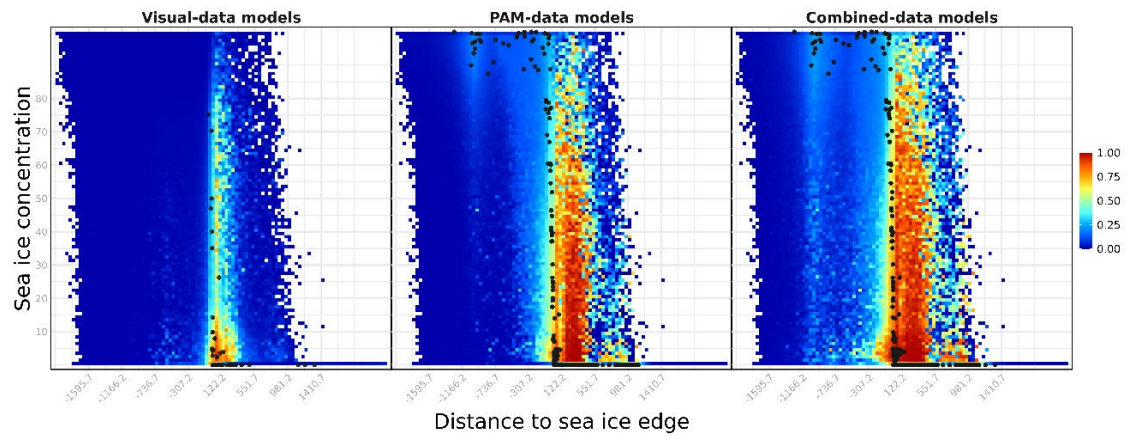
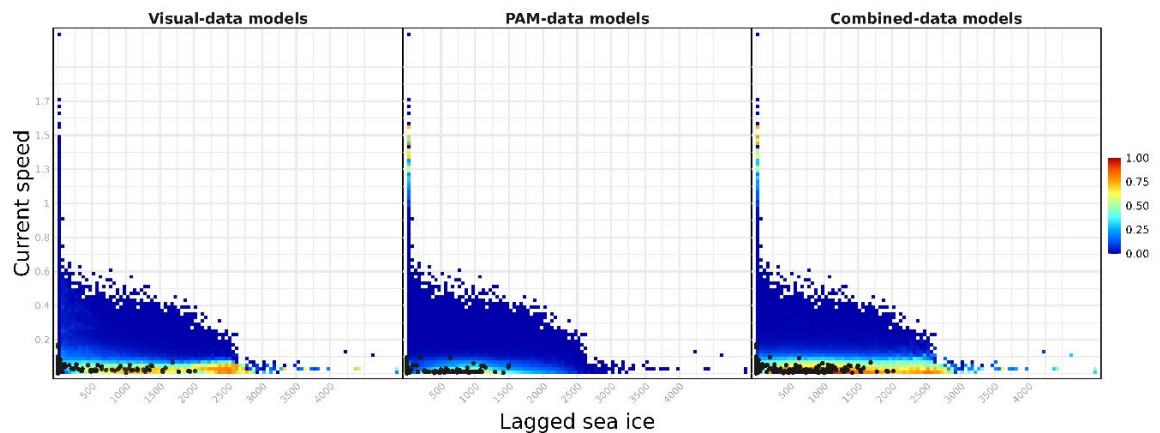
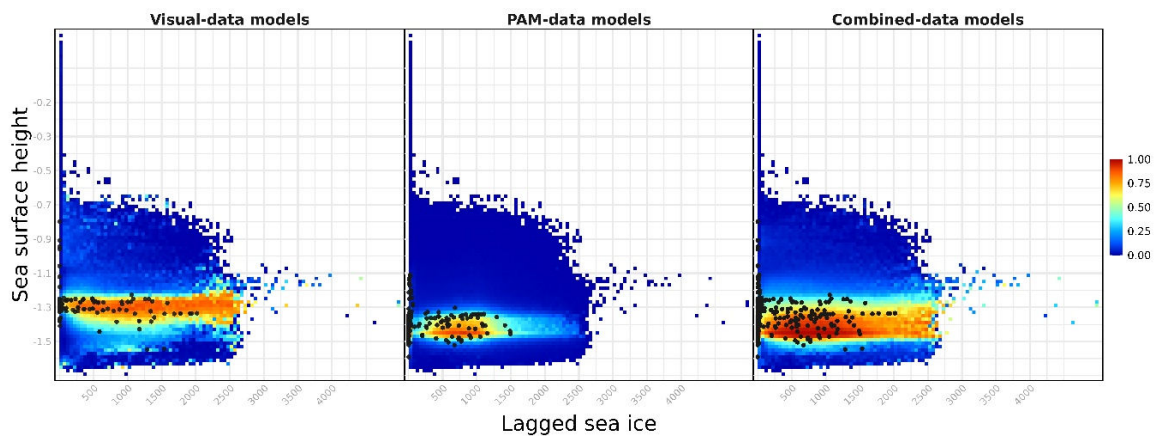
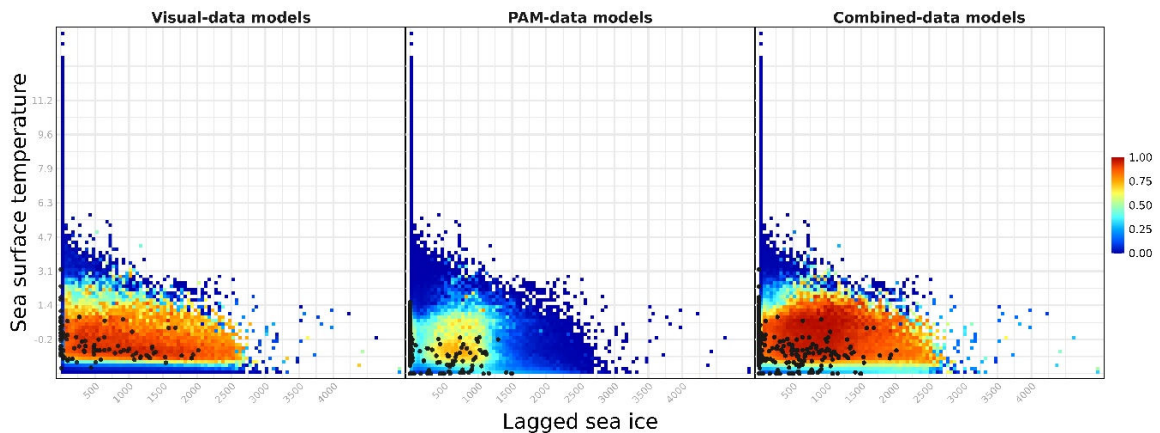
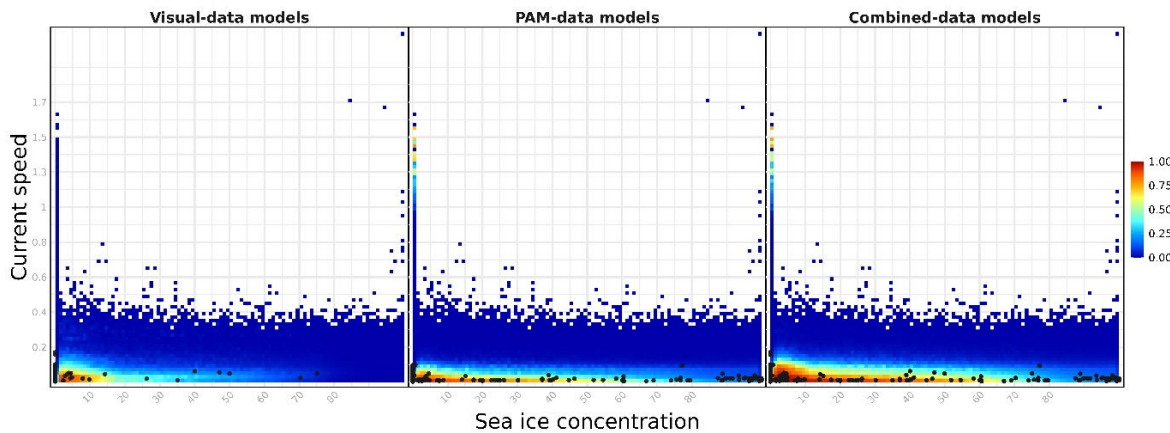


Figure S9: Single variable response curves for Antarctic blue whales’ models. To create these plots, an additional set of models was run only using one predictor in turn. Lines and shaded areas represent the mean and standard deviation of response curves on cross-validation, with different colors for each model type. In each plot, the top rugs show the spatiotemporally matched conditions at species detections (visual sighting in blue, PAM data in red), while the bottom green rug shows values at a sample of background locations from the Weddell Sea (10% of background information used to run the models). Environmental values at PAM detections, grouped by the location of acoustic stations, are shown in Figure S4. See Figure 6 for marginal response curves and Figure S10 for summary values of predicted habitat suitability in the environmental space of pairwise predictors.





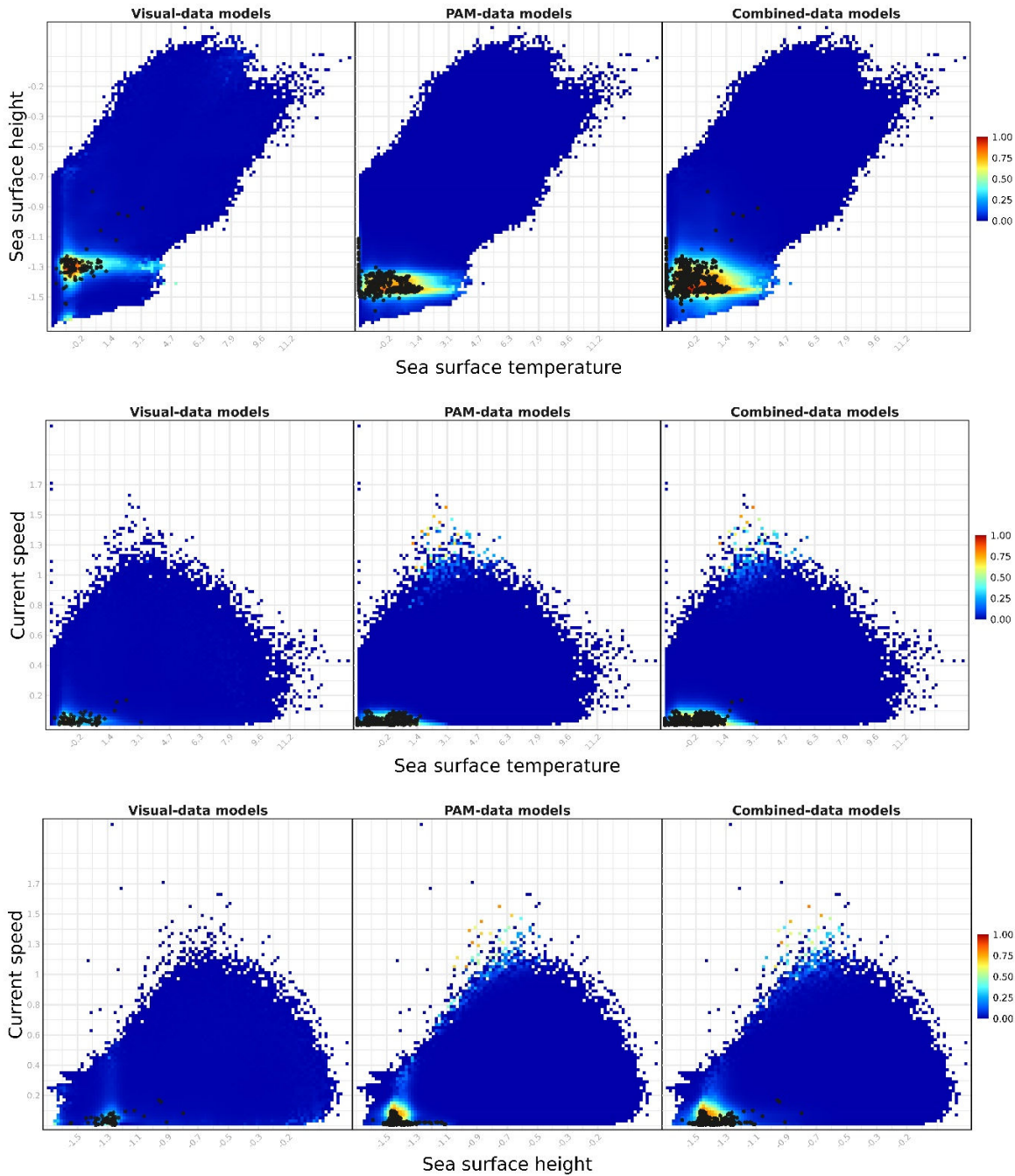


Figure S10: Predicted habitat suitability of Antarctic blue whales in pairwise environmental space of the six dynamic predictors used in the models. Columns represent the three models implemented (Model_{visual}, Model_{PAM}, and Model_{combined}, respectively). Each plot shows predicted values at year-round environmental combinations (11.7 million background locations spatiotemporally sampled from the Weddell Sea). Predictions at each combination of two predictors (represented as 100×100 pixels) were summarized to represent the 90th quantile of predicted habitat suitability per combination. Pixel colors range from blue to red (low to high habitat suitability), with white pixels for non-existent combinations in the background information. These pairwise comparisons allow all other predictors to vary together to represent pairwise habitat suitability at all other possible combinations in the study area. Spatiotemporally-matched environmental conditions at respective species detections are shown as black points.

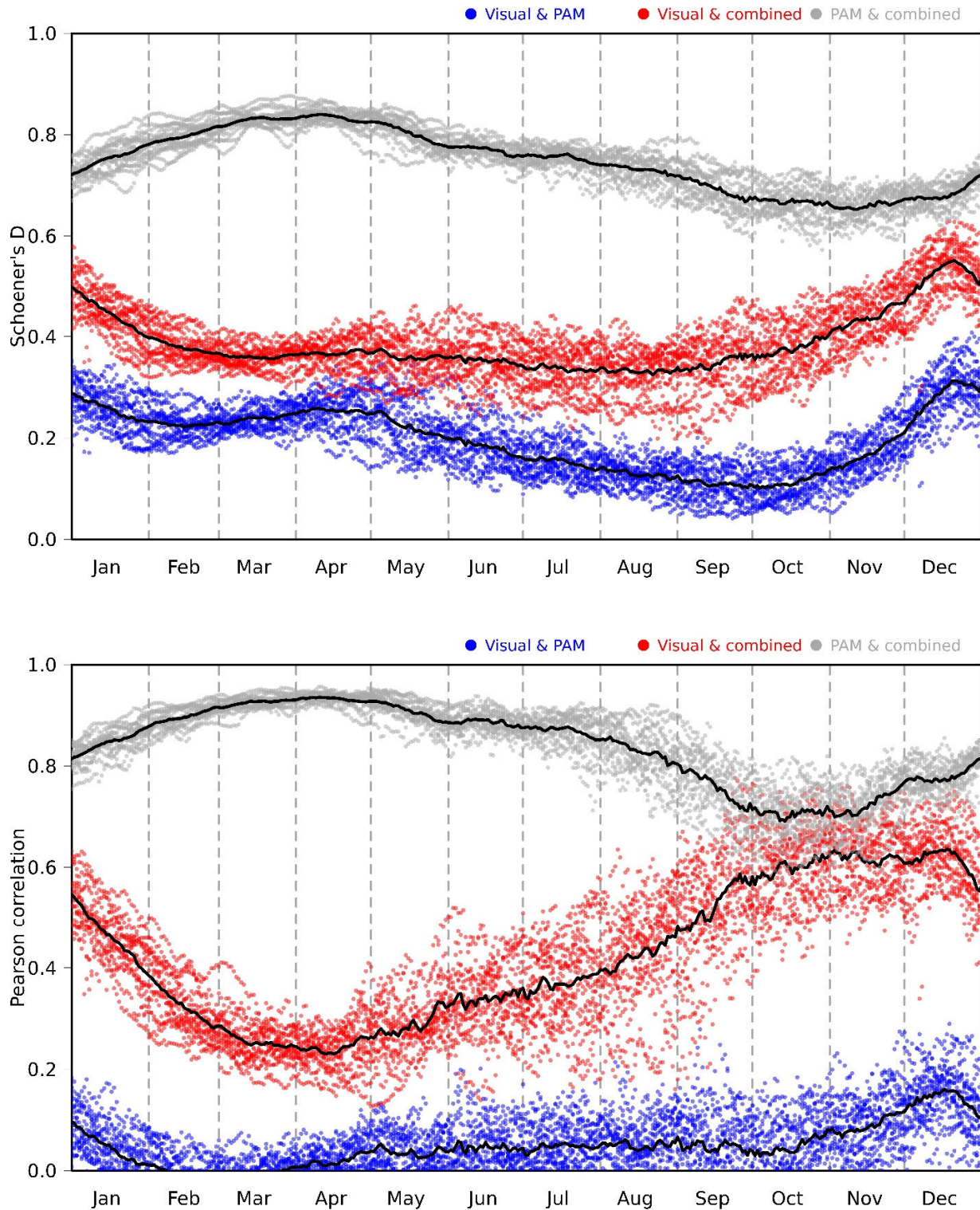
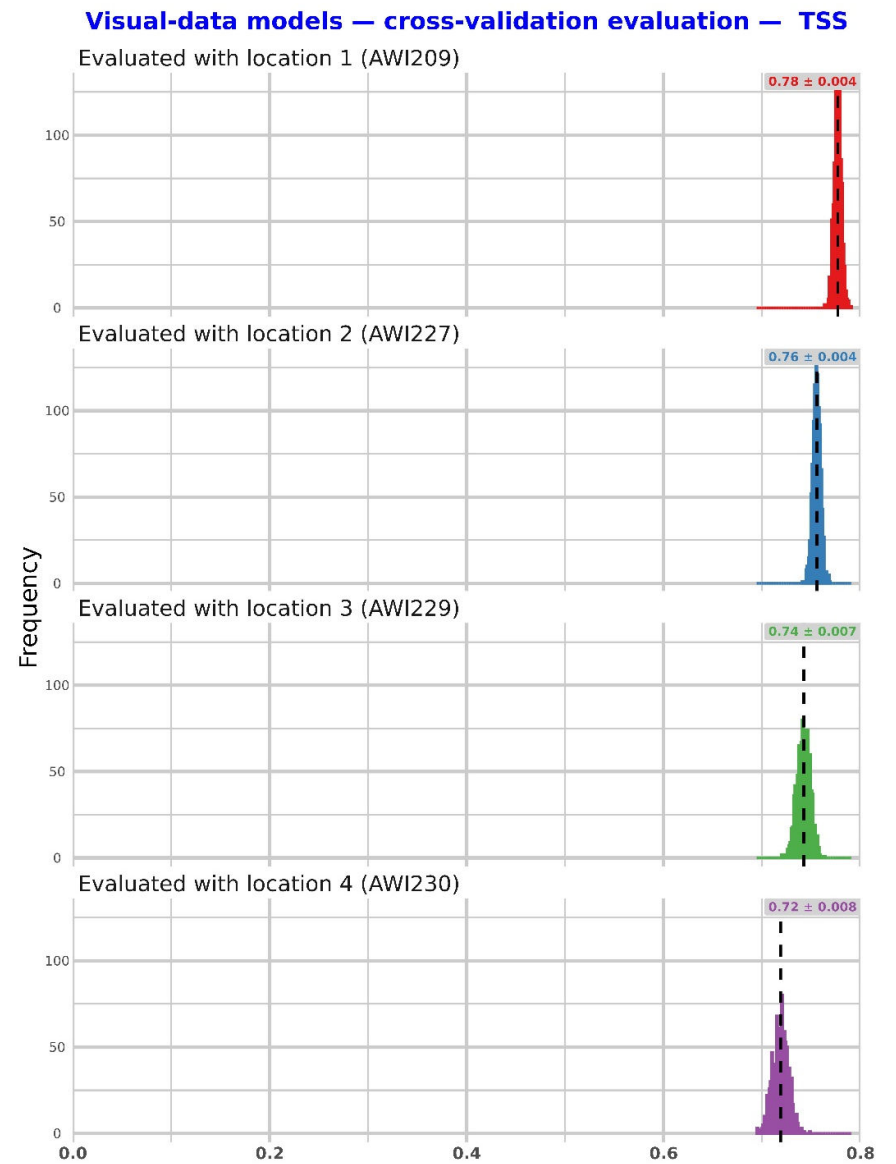
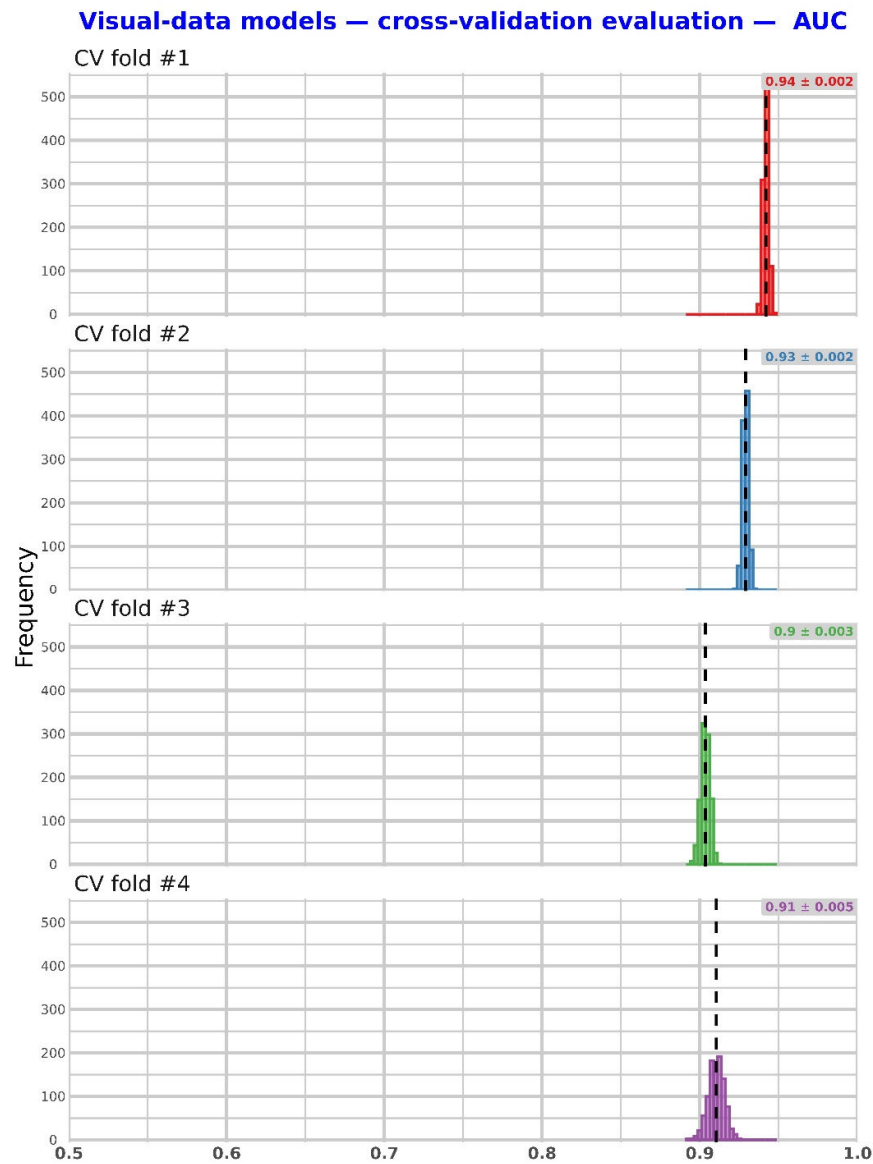
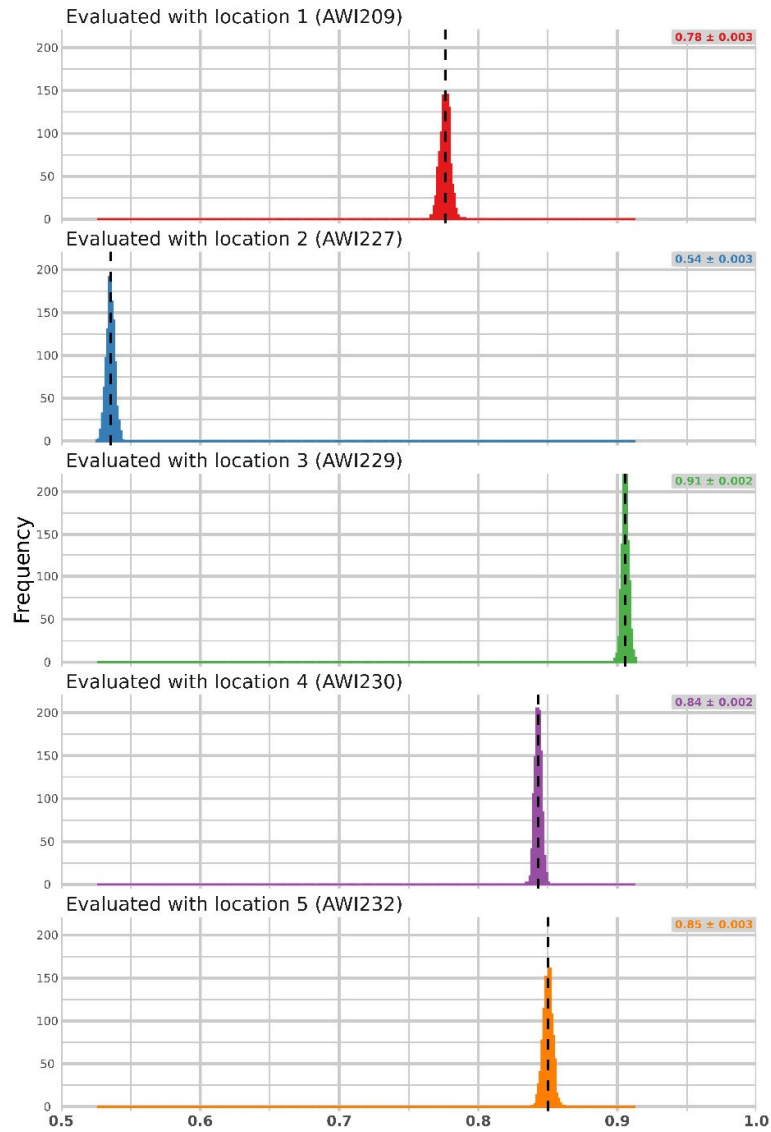


Figure S11: Spatial overlap (Schoener's D metric (Warren et al. 2008) and Pearson's correlation coefficient) between daily mean predicted habitat suitability of the three model types. Blue dots represent daily overlap values between $\text{Model}_{\text{visual}}$ & $\text{Model}_{\text{PAM}}$; red for $\text{Model}_{\text{visual}}$ & $\text{Model}_{\text{combined}}$; and grey for $\text{Model}_{\text{PAM}}$ & $\text{Model}_{\text{combined}}$. Black lines show the mean overlap value of the respective model combination for each calendar day. Schoener's D metric ranges from zero for no overlap to one for complete overlap. For similar results using Warren's I metric, see Figure 4.

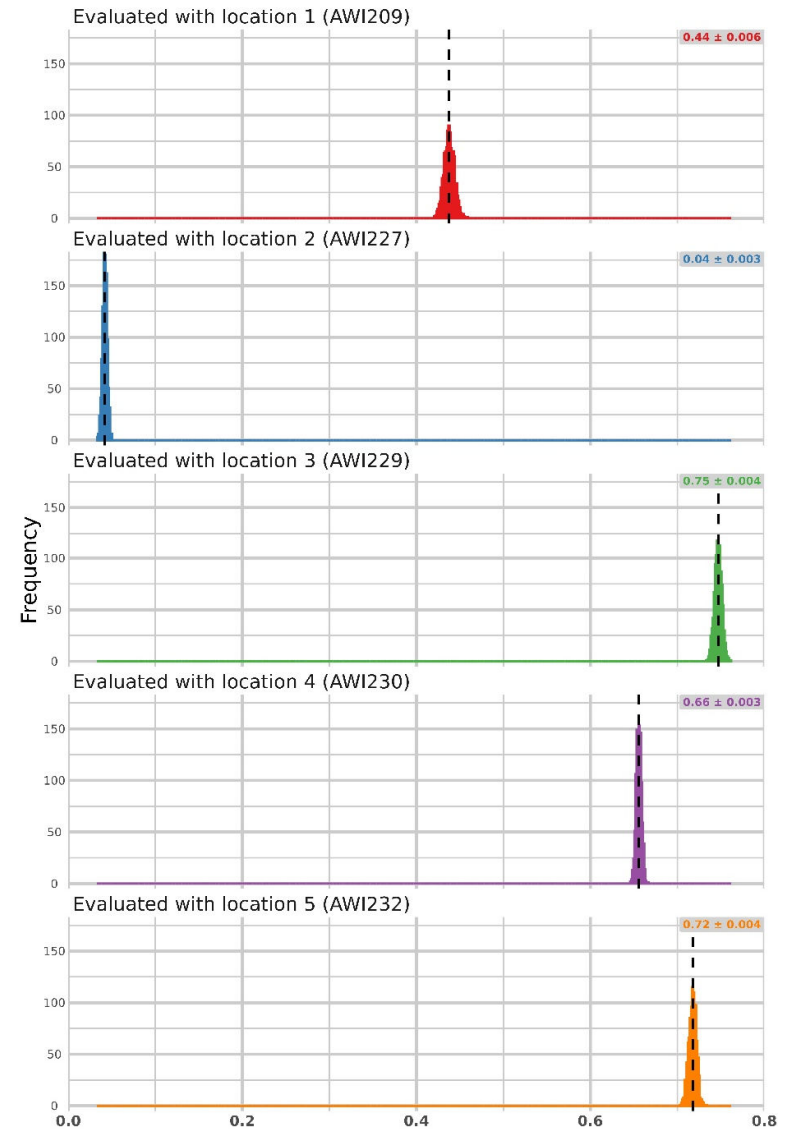


A. Visual-data models (cross-validation evaluation)

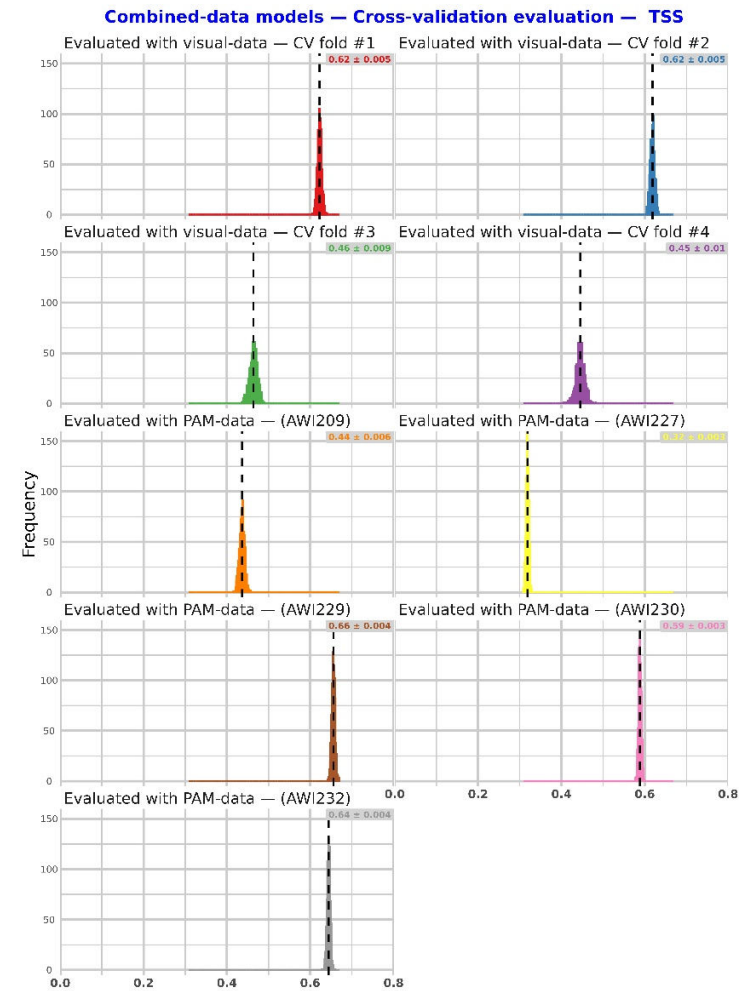
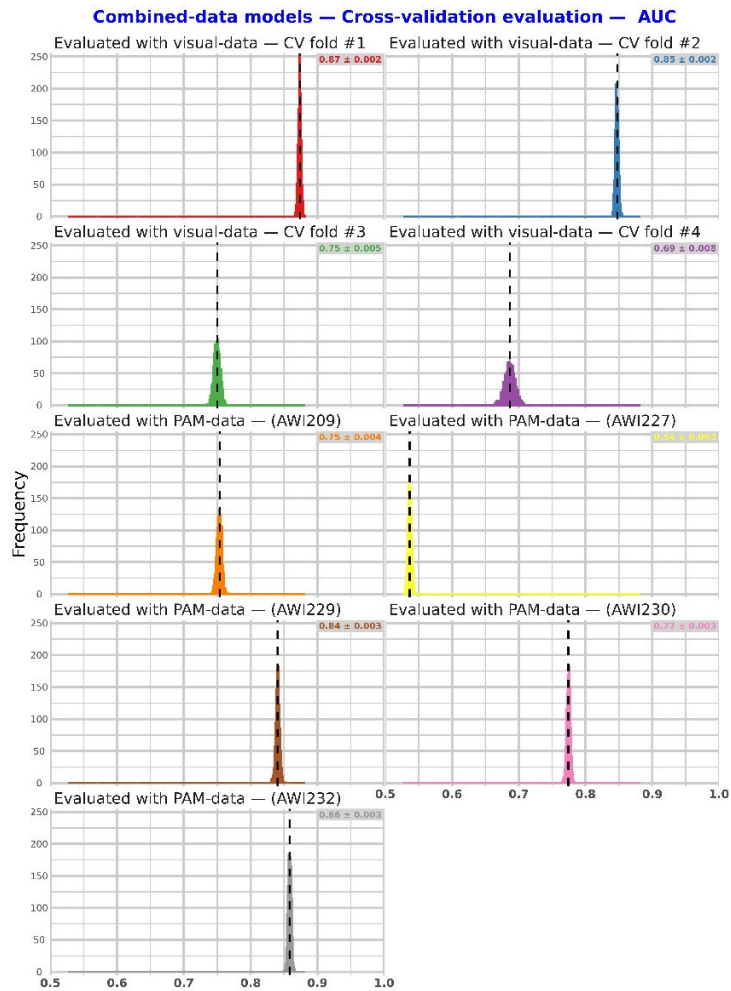
PAM-data models – cross-validation evaluation – AUC



PAM-data models – cross-validation evaluation – TSS



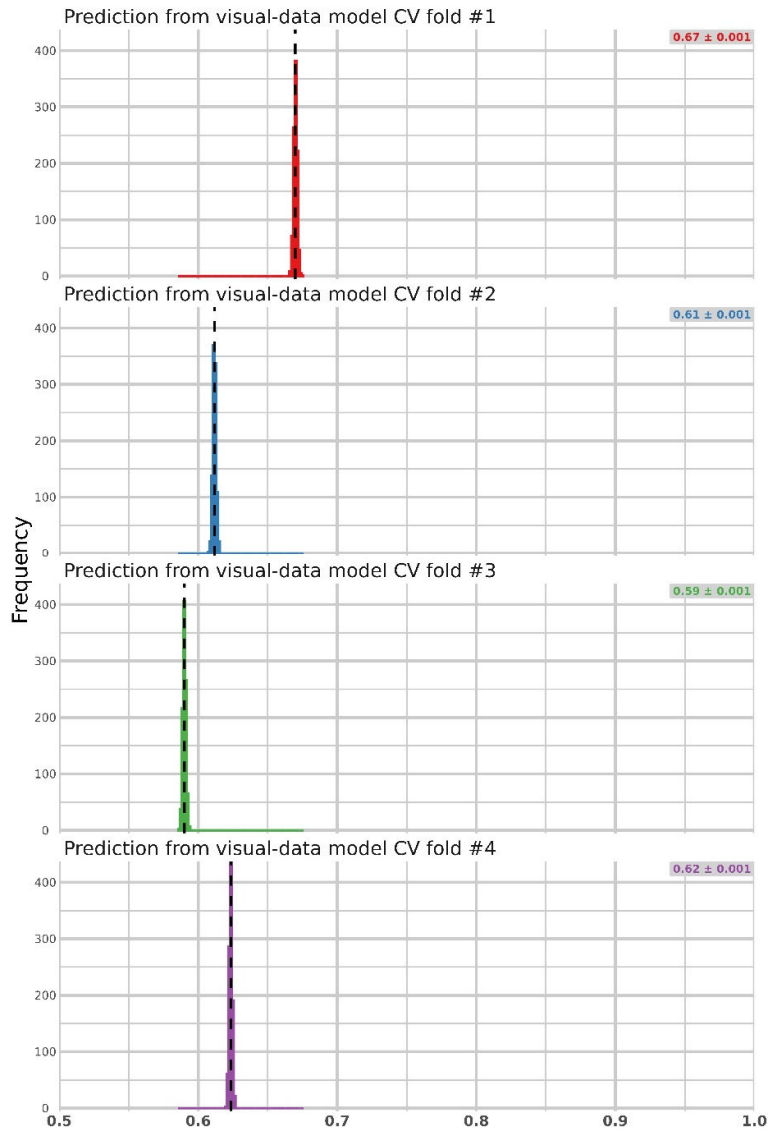
B. PAM-data models (cross-validation evaluation)



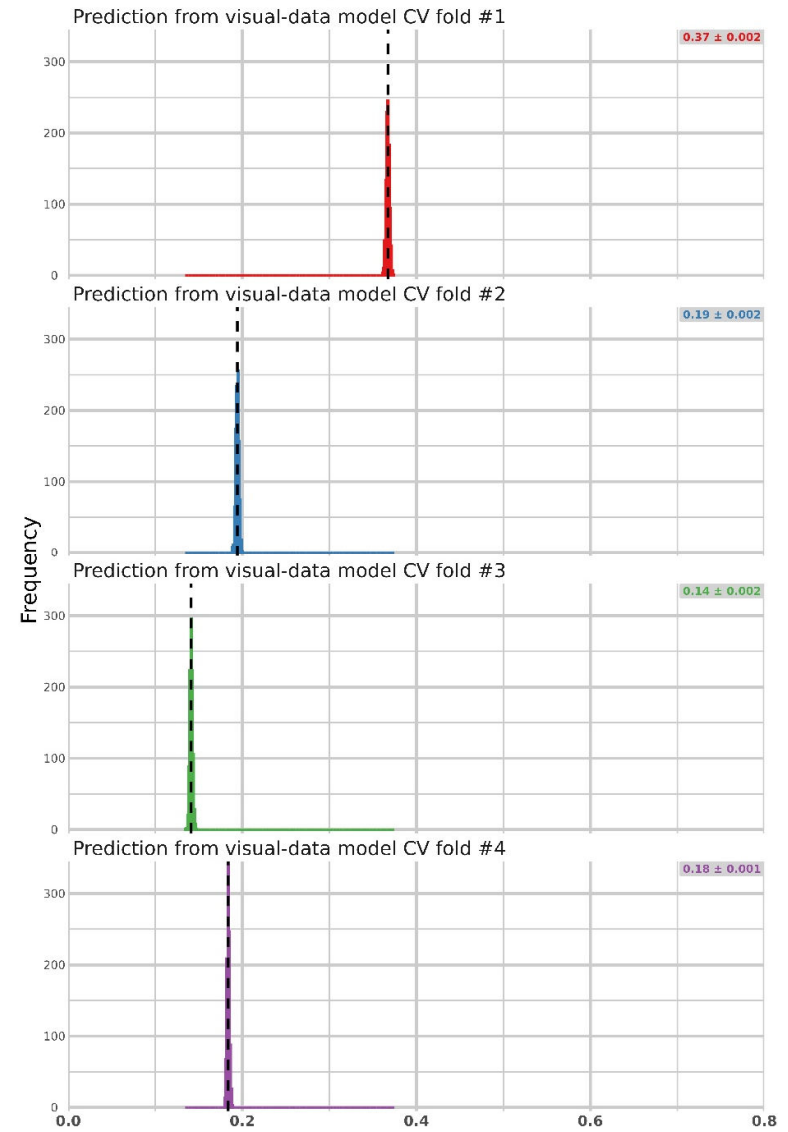
C. combined-data models (cross-validation evaluation)

Figure S12: Histograms for the calculated 1,000 raw values of cross-validated evaluation: testing AUC (left plots) and testing TSS (right plots) for (a) $Model_{visual}$; (b) $Model_{PAM}$; and (c) $Model_{combined}$. The mean and standard deviation of the metric in the respective model and cross-validation fold is shown in the top right of each plot; the mean value is shown as a vertical dashed line. The overall summary of the evaluation metrics is shown in Table 2. For more information on the spatial blocks used to cross-validate $Model_{visual}$, see Figure S5. The location of the PAM stations used to cross-validate $Model_{PAM}$ is shown in Figure 1.

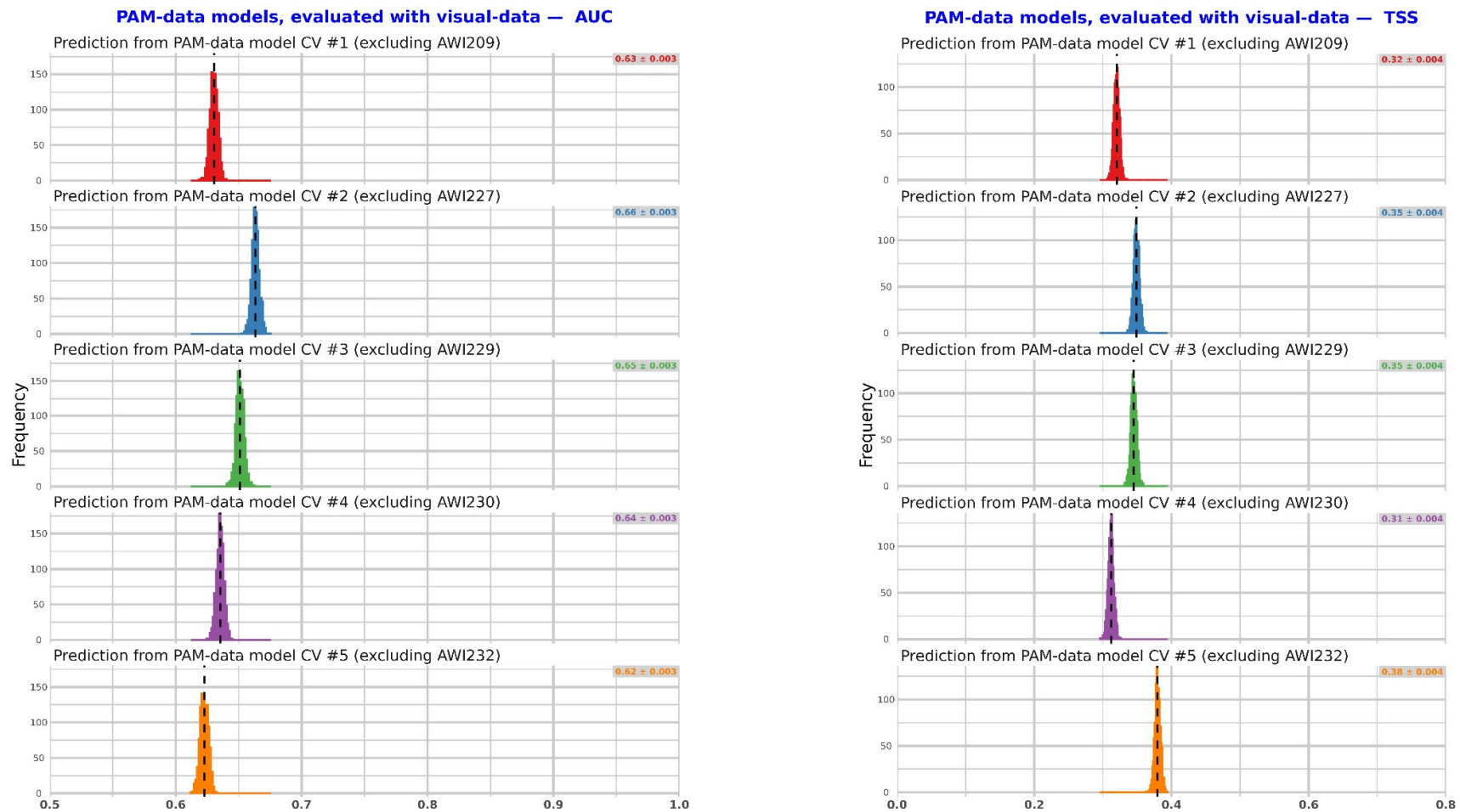
Visual-data models, evaluated with PAM-data — AUC



Visual-data models, evaluated with PAM-data — TSS



A. Visual-data models, evaluated with PAM data



B. PAM-data models, evaluated with visual data

Figure S13: Histograms for the calculated 1,000 raw values of external evaluation: testing AUC (left plots) and testing TSS (right plots) for (a) cross-validated visual-data models ($\text{Model}_{\text{visual}}$), evaluated with independent PAM data; (b) cross-validated PAM-data models ($\text{Model}_{\text{PAM}}$), evaluated with independent visual sightings data. The mean and standard deviation of the metric in the respective model and cross-validation fold is shown in the top right of each plot; the mean value is shown as a vertical dashed line. The overall summary of the evaluation metrics is shown in Table 2. For more information on the spatial blocks used to cross-validate $\text{Model}_{\text{visual}}$, see Figure S5. The location of the PAM stations used to cross-validate $\text{Model}_{\text{PAM}}$ is shown in Figure 1.

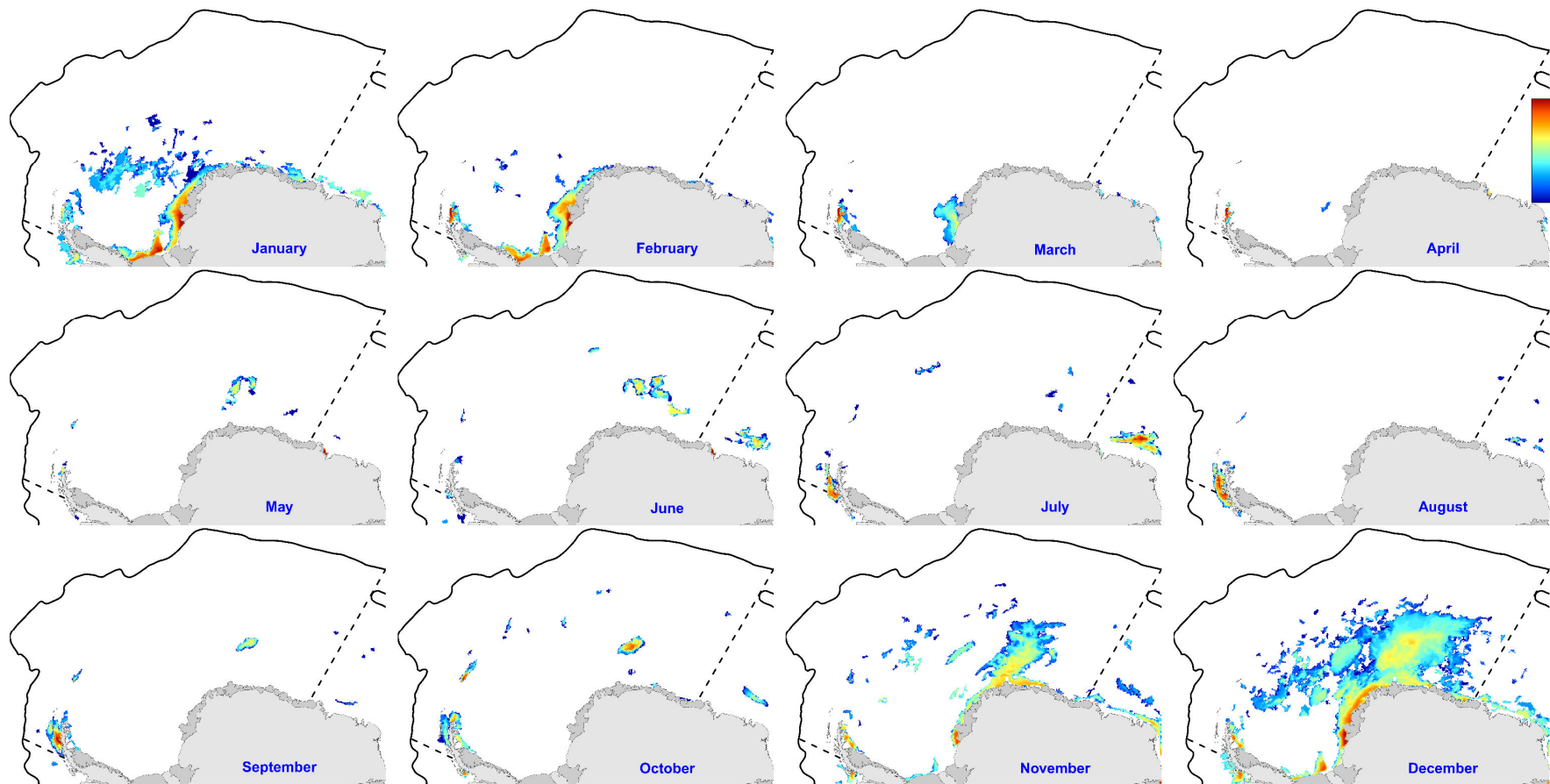
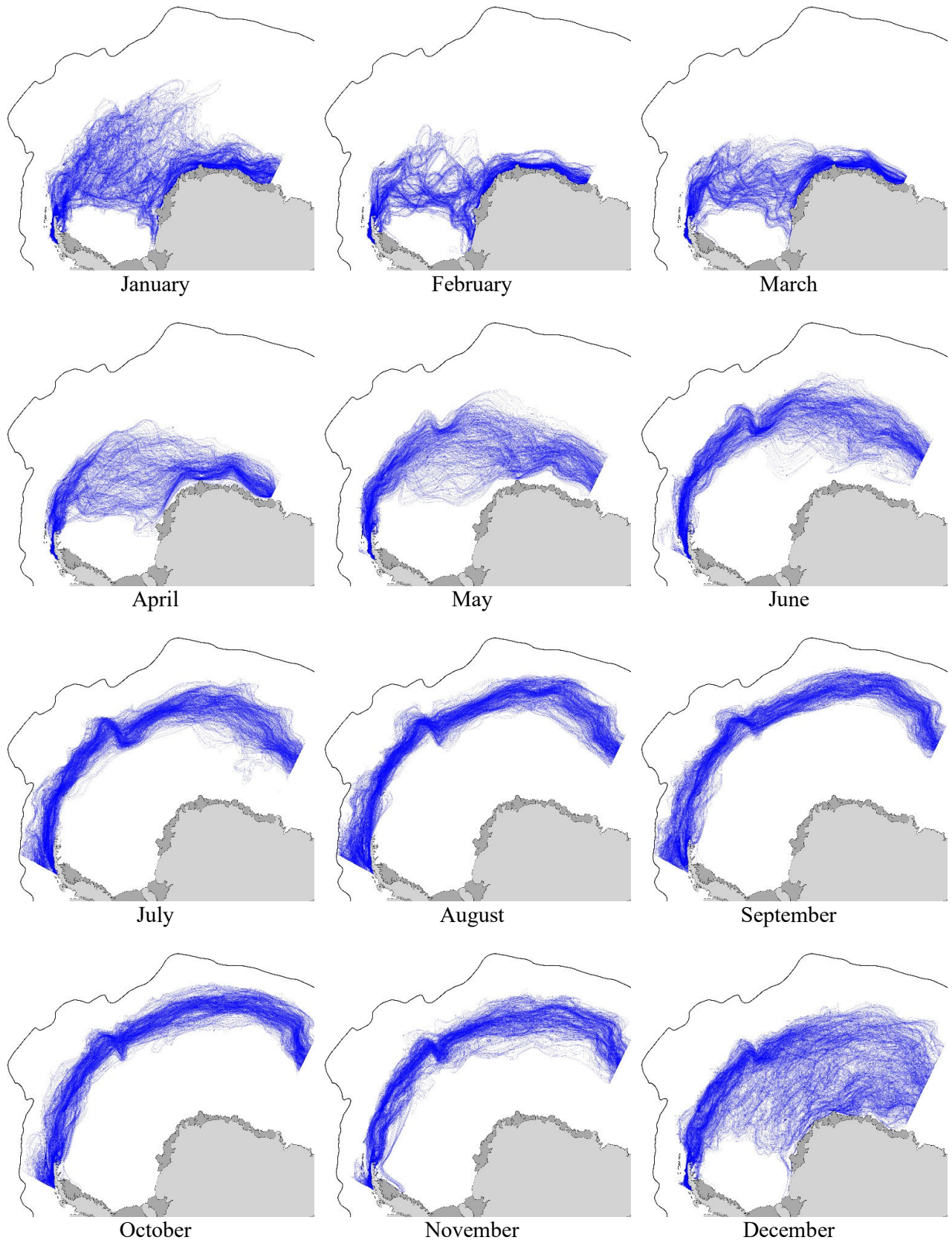


Figure S14: Number of days (\log_{10} scale) each cell was identified as polynya (2003-2019). Daily polynyas (areas with SIC $\leq 15\%$ south of the SIE) were determined by two rules: ≥ 20 connected cells ($>2,000$ km²) and persistent for at least five consecutive days (two days before and two days after each selected day); see El-Gabbas et al. 2021a for more details. Daily polynyas were converted into a daily binary map (polynya/non-polynya); then, for each cell and month combination, the number of days intersected with polynyas was identified. For the location of the SIE in the respective month, see Figure S15.



(A)

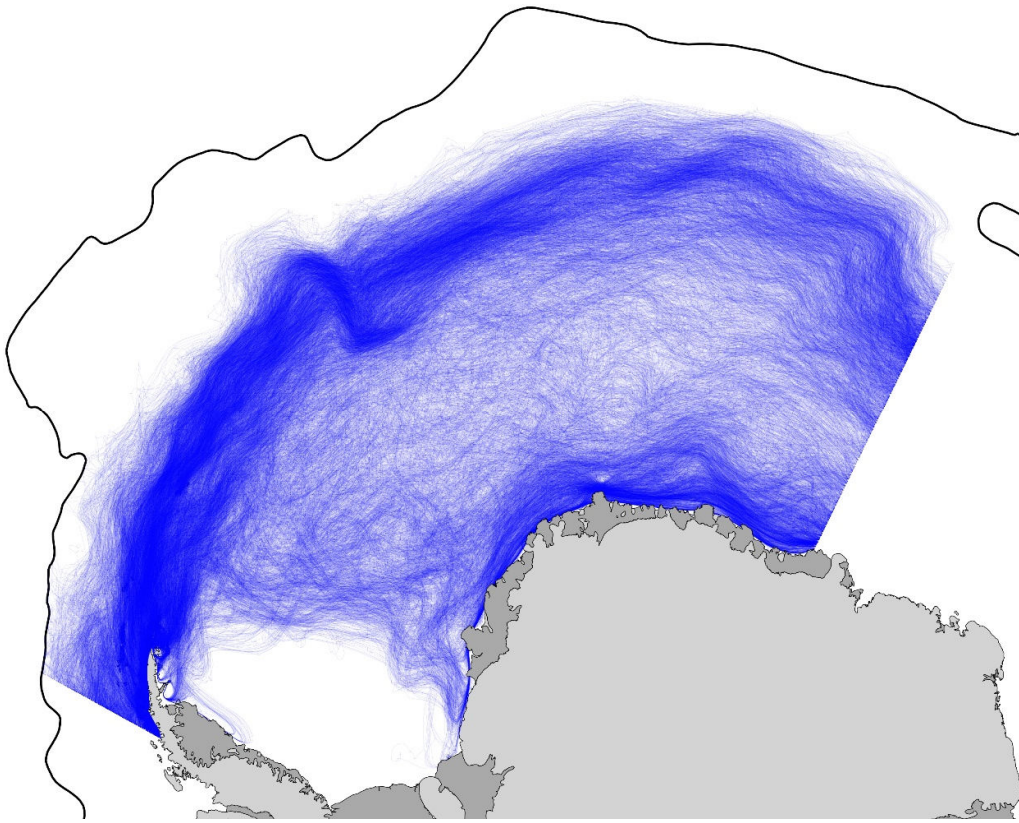
**(B)**

Figure S15: The estimated location of daily sea ice edge from 2003 to 2019 in each month (a) and irrespective of the month (b). The area south of the Weddell Basin is permanently covered with high sea ice (sea ice concentration $>15\%$ during the whole period), except near the Brunt and Larsen Ice Shelves. This area was predicted unsuitable for the Antarctic blue whales in all models, except sporadically off the Brunt Ice Shelf.

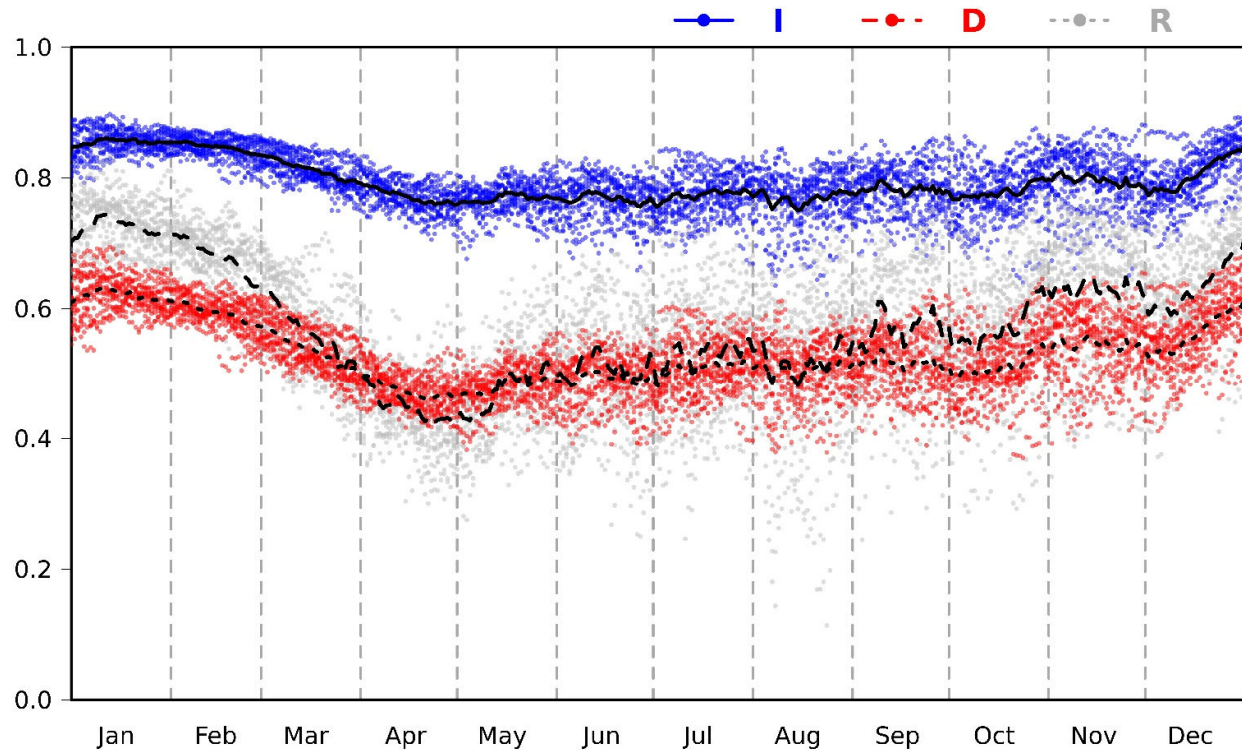
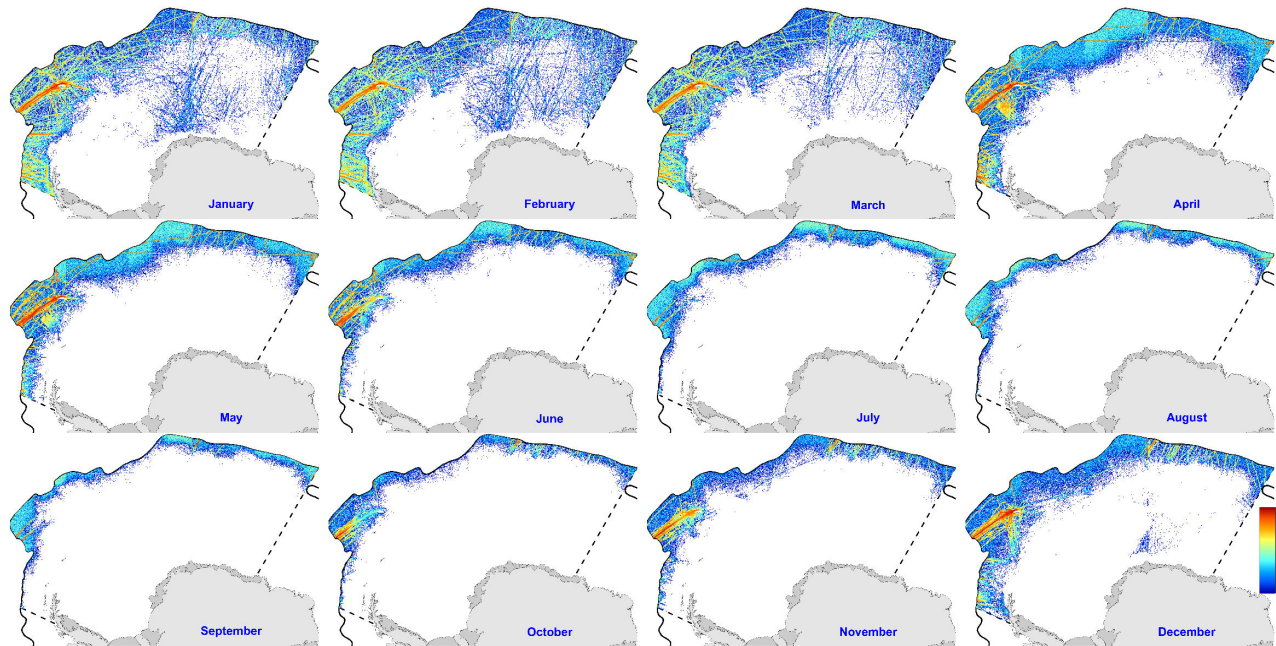
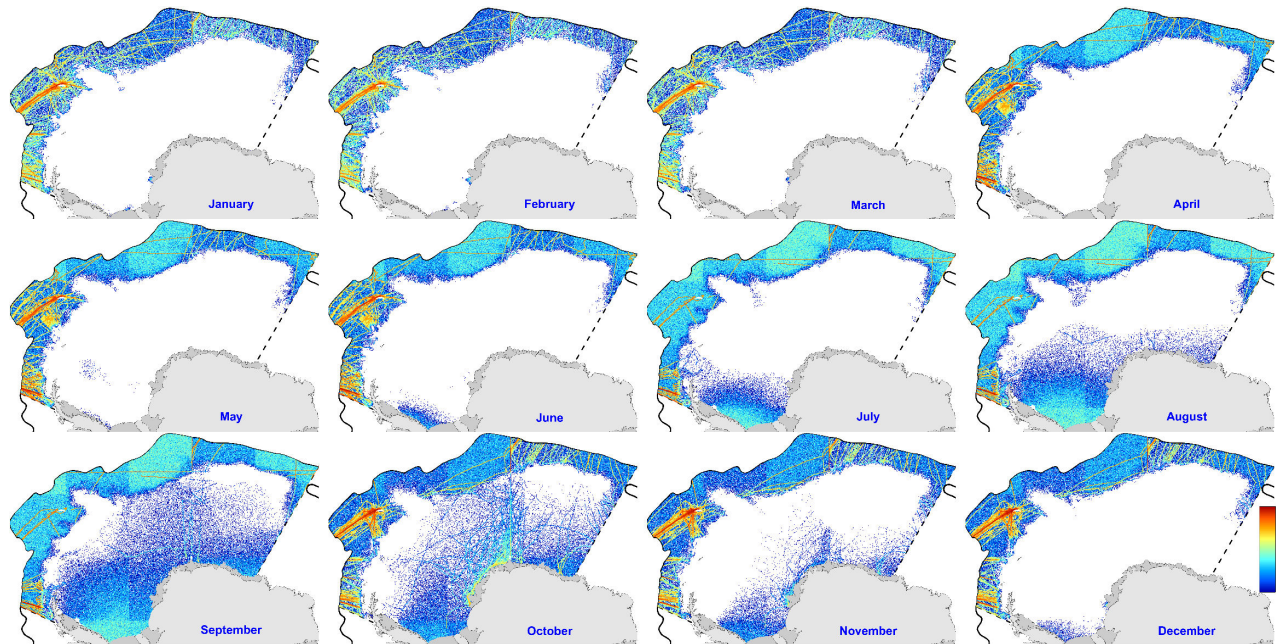


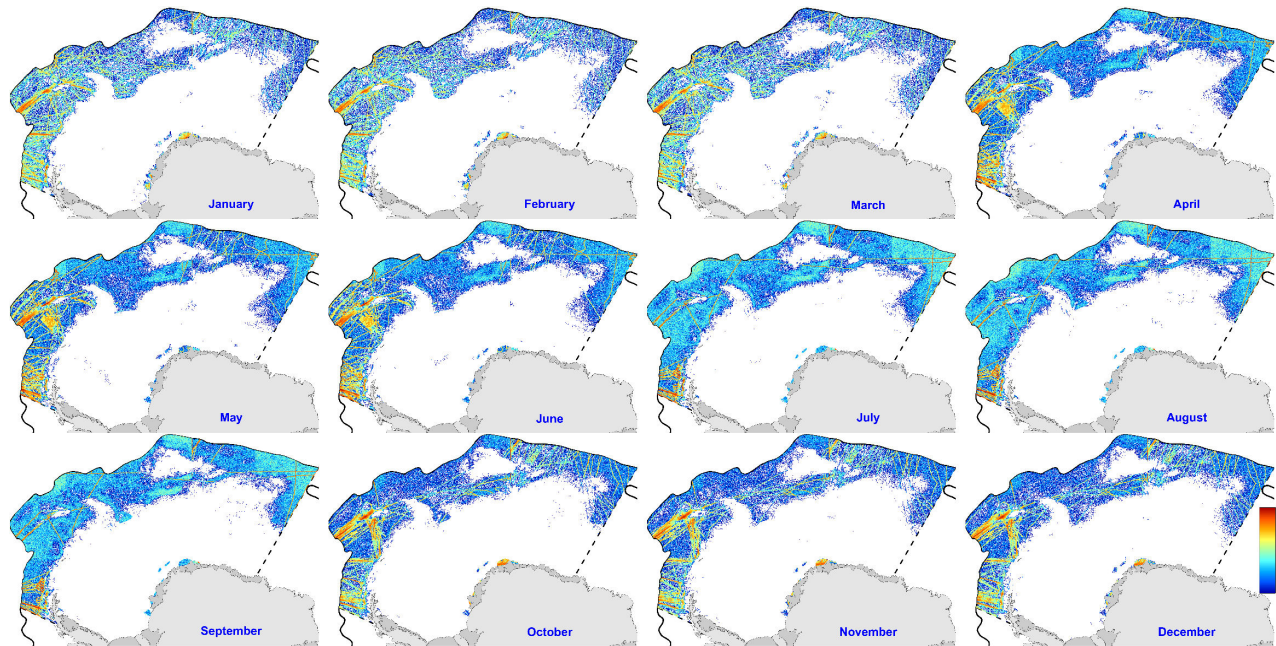
Figure S16: Spatial overlap between daily mean predicted habitat suitability of the Antarctic blue whales in the Weddell Sea visual sightings (**D**: Schoener's D metric; **I**: Warren's I (Warren et al. 2008) and **R**: Pearson's correlation coefficient). This plot dictates the overlap between 1) models run in the Weddell Sea using only dynamic predictors (this study, $\text{Model}_{\text{visual}}$) and 2) models that used circum-Antarctic visual sightings along with both static and dynamic predictors (El-Gabbas et al. 2021a), cropped to the Weddell Sea study area. Dots represent daily overlap values between models, while lines show the mean overlap value for each calendar day. Values of **D** and **I** range from zero for no overlap to one for complete overlap.



(A) SST > 1.6°C



(B) SSH > -1.1m



(C) Current speed > 0.1

Figure S17: Number of background locations used to train the models (\log_{10} scale) at environmental conditions beyond values at acoustic presences: (A) SST $> 1.6^{\circ}\text{C}$; (B) SSH $> -1.1\text{m}$; and (C) Current speed $> 0.1 \text{ ms}^{-1}$. These plots explain, for example, why models predicted low HS values north of the sbACC. These areas have environmental conditions beyond conditions at mooring stations.

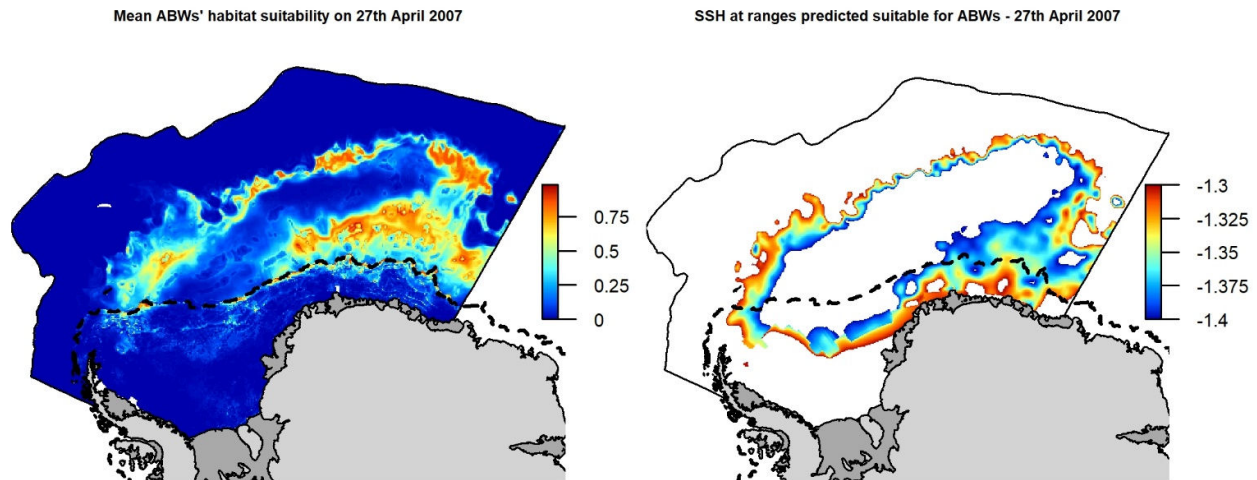
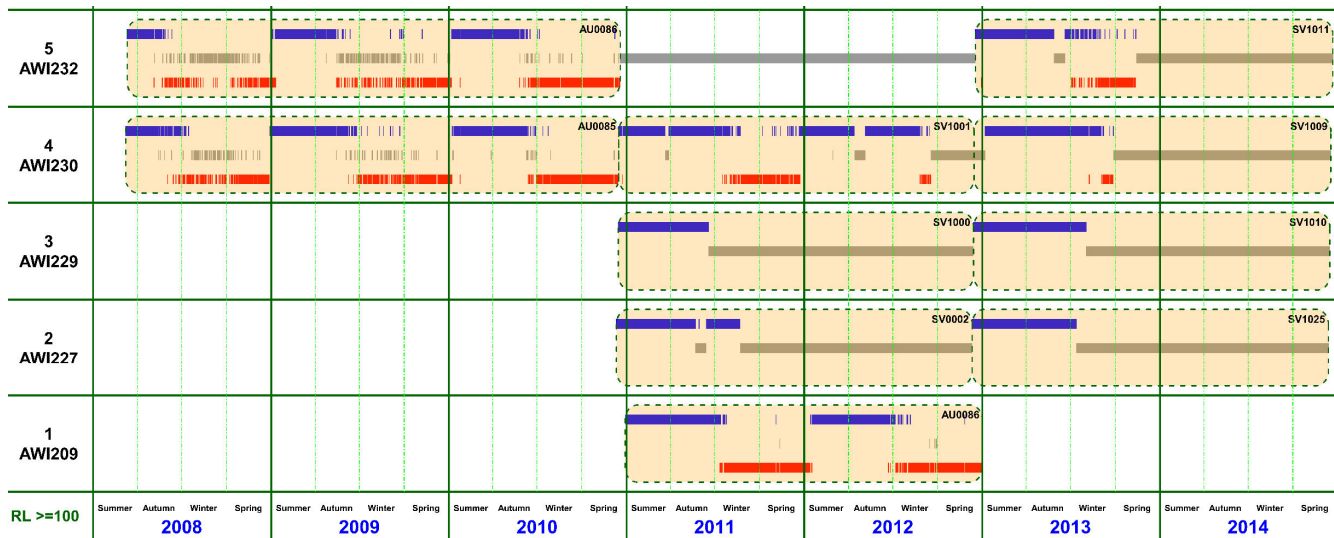
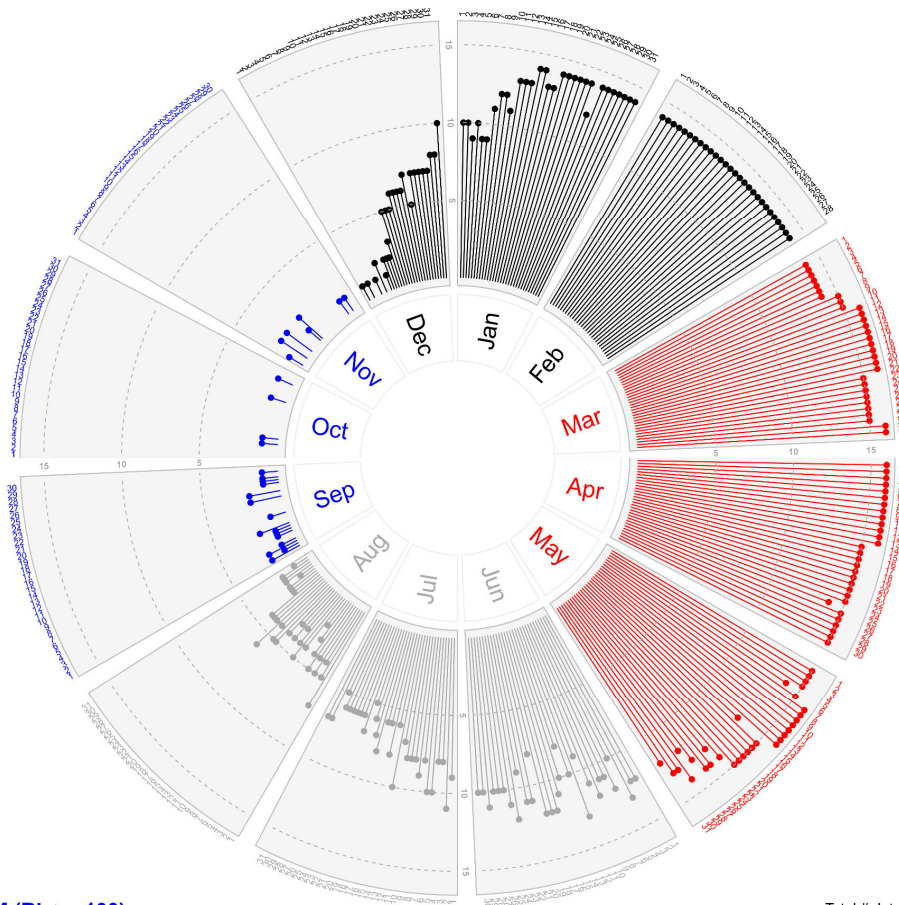


Figure S18: The left map shows mean predicted ABWs' habitat suitability on 27th April 2017. The right plot represents SSH on the same day. Only SSH values within the range identified as suitable by Model_{PAM} are plotted (between -1.4 to -1.3 m [see Figure 6]; areas beyond this range are shown in white). The estimated location of the SIE on this day is shown as a dashed line on both maps. SSH was always among the two most important predictors (Figure 5).

This figure to the right can (partially) explain the pattern of suitable habitats in the left figure: the low band of HS between 60° S and 62° S (overlapping with the location of Weddell Gyre) and areas in the northern part of the study area (to the north of the sbACC), which have SSH values beyond the suitable range for ABWs (as identified by Model_{PAM}).



(A)



PAM (RL >= 100)

Total # detections: 2992
Maximum per day: 16

(B)

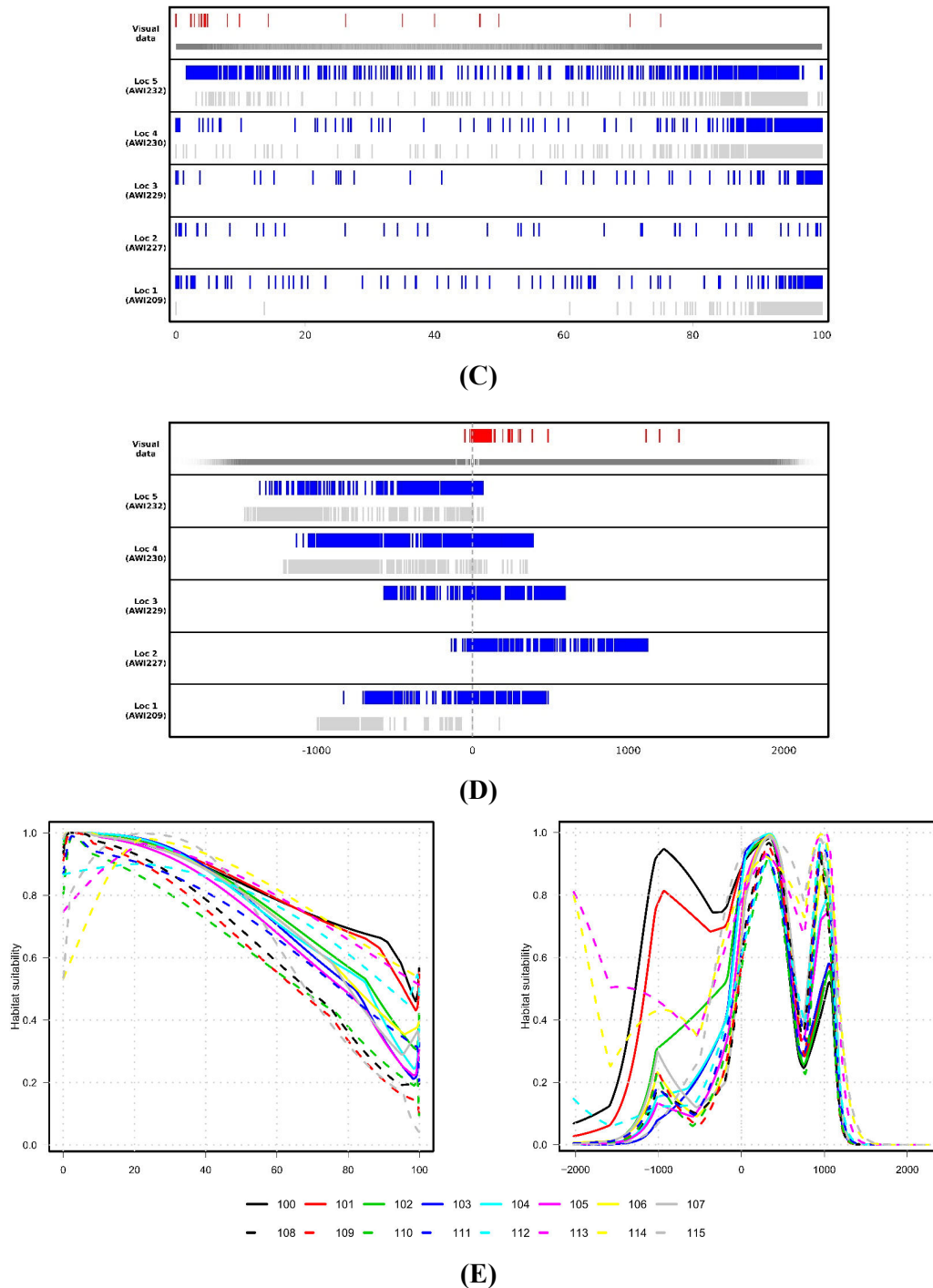


Figure S19: Antarctic blue whale PAM data using RL threshold ≥ 100 dB. Panels **A** and **B** show the temporal distribution of acoustic presences. Panels **C** and **D** show values of SIC and distance to SIE, respectively, at ABW acoustic detections, using the same RL threshold. Panel **E** shows marginal response curves for SIC (left) and distance to SIE (right) using different values of RL (100-115 dB). In panel **E**, different models were fit using the respective acoustic presences without cross-validation. A low RL threshold (\sim larger detection ranges) resulted in larger sample size (compare **A** with Figure 2 and **B** with Figure S1b), covering a much broader range of SIC values and distance to the SIE (compare **C-D** with Figure S4). The use of small RL threshold (i.e., long distances) led to higher HS at high SIC and at locations much south (c.a. 1000km) of the SIE. This figure highlights the importance of the careful choice of RL threshold and the resulted environmental mismatch of considering calls at much long distances from the recording sites as presences. More details on the recorders are shown in Table 1 and Figures 1-2.

Appendix 1

Sources of visual sightings data

- Burkhardt, Elke (2011): Whale sightings during POLARSTERN cruise ANT-XXVII/2. Alfred Wegener Institute, Helmholtz Center for Polar and Marine Research, Bremerhaven, PANGAEA, <https://doi.org/10.1594/PANGAEA.760340>
- Burkhardt, Elke (2012): Whale sightings during POLARSTERN cruise ANT-XXVII/3. Alfred Wegener Institute, Helmholtz Center for Polar and Marine Research, Bremerhaven, PANGAEA, <https://doi.org/10.1594/PANGAEA.783806>
- Burkhardt, Elke (2013): Whale sightings during POLARSTERN cruise ANT-XXVIII/2. Alfred Wegener Institute, Helmholtz Center for Polar and Marine Research, Bremerhaven, PANGAEA, <https://doi.org/10.1594/PANGAEA.819861>
- Burkhardt, Elke (2013): Whale sightings during POLARSTERN cruise ANT-XXIX/2. Alfred Wegener Institute, Helmholtz Center for Polar and Marine Research, Bremerhaven, PANGAEA, <https://doi.org/10.1594/PANGAEA.819866>
- Burkhardt, Elke (2020): Whale sightings during POLARSTERN cruise PS96 (ANT-XXXI/2). Alfred Wegener Institute, Helmholtz Centre for Polar and Marine Research, Bremerhaven, PANGAEA, <https://doi.org/10.1594/PANGAEA.923113>
- Cheeseman, T. and K. Southerland. (2021). Happywhale encounters.
- Happywhale (2021) Happywhale - Blue Whale in South Atlantic Ocean. Data downloaded from OBIS-SEAMAP (<http://seamap.env.duke.edu/dataset/1759>) and originated from Happywhale.com.
- Happywhale (2021) Happywhale - Blue Whale in Southern Ocean. Data downloaded from OBIS-SEAMAP (<http://seamap.env.duke.edu/dataset/1760>) and originated from Happywhale.com.
- Herr, Helena; Siebert, Ursula (2018): Aerial cetacean survey Southern Ocean 2012/2013. PANGAEA, <https://doi.pangaea.de/10.1594/PANGAEA.894914>
- Herr, Helena; Viquerat, Sacha; Siebert, Ursula (2018): Ship based cetacean survey Southern Ocean 2014/2015. PANGAEA, <https://doi.pangaea.de/10.1594/PANGAEA.894873>
- iNaturalist contributors, iNaturalist (2022). iNaturalist Research-grade Observations. iNaturalist.org. Occurrence dataset <https://doi.org/10.15468/ab3s5x> accessed via GBIF.org. <https://www.gbif.org/occurrence/2634034610>